Chapter 4

Molecular Mechanisms Behind The Regulation Of Cell Cycle Progression In Cardiovascular System

Kazushi Urasawa, M.D., and Akira Kitabatake, M.D.

1. Introduction

Percutaneous coronary intervention (PCI) is widely performed as an useful and indispensable technique to treat the patients with ischemic heart diseases such as angina pectoris and acute myocardial infarction. However, a major limitation of this powerful technique is the fact that roughly 40% of patients undergoing balloon angioplasty have developed the coronary restenosis, recurrence of stenosis at the site of angioplasty several months after the procedure[1]. It is well known that the coronary restenosis is composed of several independent vascular events such as elastic recoil, vascular remodeling and smooth muscle cell (SMC) proliferation. Intra-coronary stents have proven to be effective to reduce the coronary restenosis caused by elastic recoil and chronic vascular remodeling. The restenosis rate after stenting, however, is still as high as 20%[2]. And, in these stent cases, SMC proliferation is the major cause of restenosis.

Various growth factors and cytokines are playing pivotal roles in the process of coronary restenosis, which includes SMC migration, proliferation, and extracellular matrix production from SMC[3]. In general, growth factors and cytokines are recognized by cell surface receptors, and the activated receptors then trigger several intracellular signaling cascades finaly resulting in cell cycle progression[4]. Any points within this signaling cascade could be the target to prevent SMC growth in the setting of coronary restenosis. Based on this hypothesis, we introduce two distinct approaches to control SMC growth in this chapter. First, the effect of suramin, a potent anti-growth factor agent with broad spectrum, on the growth of cultured SMC. Secondly, the effect of adenovirus vector containing cyclin-dependent kinase inhibitor (p57Kip2) gene, on neointimal hyperplasia after vascular injury. Then, a possible mechanism of cell-cycle control in SMC is discussed.

2. Vascular Smooth Muscle Cell Proliferation Was Effectively Suppressed by Non-specific Growth Factor Inhibitor, Suramin.

The purpose of this study is to investigate the effect of non-specific growth factor inhibitor, suramin, on smooth muscle cell proliferation *in vitro* and *in vivo*.

Methods

Cell isolation and culture: A10 cells, an established smooth muscle cell line which was originated from rat abdominal aorta, were maintained in DMEM supplemented

with 10% FBS, 100mg/ml penicillin and 100mg/ml streptomycin. The A10 cells used for this study were those maintained for less than 60 days. In order to establish the primary culture of rat vascular SMC (RVSMC), abdominal aortae were excised from male Wistar rats (250-400 gram body weight), dissected into small pieces (about 1mm length), then placed on tissue culture dishes containing DMEM supplemented with 20% FBS. Two to three weeks after the tissue preparation, aortic rings were removed from the dishes, and the RVSMC grown from dissected tissues were passaged by trypsinization. All experiments on RVSMC were performed between passage 3 to 6.

Treatment of vascular smooth muscle cells with suramin: A10 or RVSMC were cultured in DMEM supplemented with 10% FBS until cellular density was reached to 50%. Then, culture medium was exchanged to DMEM containing 0.5% FBS, and maintained for following 48 (or 24) hours in order to synchronize the cell-cycle to G0/1 phase. The synchronized cells were stimulated either by 10ng/ml PDGF-AA, PDGF-AB, PDGF-BB or 2% FBS for 24 hours. PDGF- or serum-stimulated DNA synthesis was assessed by measuring [^{3}H] -thymidine uptake. In detail, after the growth stimulation by PDGF or serum, cells were washed by DMEM twice, then incubated with DMEM containing 1mCi/ml [^{3}H] -thymidine for one hour. These cells were fixed in 6% trichloroacetic acid at 4°C for 12 hours, treated with 1N NaOH at 37°C for 1 hour, then neutralized by adding 6N HCl. Extracted radioactivity was measured by liquid scintillation counter.

Animal model of neointimal formation: Japanese white rabbits (weighing 2.5 to 3.0 kg) were anesthetized with sodium pentobarbital (25mg/kg, intravenously). Catheter introducer sheath with 7cm length (4F Super-sheath, Medikit, Japan) was introduced into right femoral artery. A 0.014 inch guide wire (High-Torque Floppy II, ACS, Temecula, USA) was advanced to right common carotid artery through the catheter introducer sheath under fluoroscopic guide. Then, a coronary angioplasty balloon catheter with 3mm diameter and 10mm length (ACX-II, ACS, Temecula, USA) was advanced over the guide wire to the distal end of right common carotid artery and inflated at 120 psi. Endothelial layer of the common carotid artery was denuded by passing the inflated balloon three times.

Local delivery of suramin in the animal model: After the balloon-mediated vascular endothelial denudation, an angioplasty balloon catheter was exchanged to a porous balloon catheter (Transport, Cardio Vascular Dynamics. Inc., Irvine, USA). This catheter is composed of dual balloons which are located within one another; inner dilating balloon and outer infusion balloon. The outer infusion balloon has forty-eight small pours (250μm in diameter) circumfearentially across 10mm of its mid section to permit regional infusion of various pharmacological agents. At the site of endothelial denudation, inner balloon of Transport was inflated with 90 psi, then pressure was reduced to 15 psi. Suramin dissolved in 5% glucose was injected through the drug delivery channel of the Transport catheter at the constant infusion rate of 30ml/hour over 10 minutes using an automatic infusion pump. Two differ-

ent concentration of suramin solutions (0.5mM and 1.0mM) were injected into three (low dose group) and six rabbits (high dose group), respectively. In six rabbits, 5% glucose was injected in the same manner (control group).

Evaluation of Intimal Hyperplasia: Three weeks after the procedure, arterial segments between two anatomical makers (mandibula and subclavia) were excised, washed with PBS, then fixed in 8% formaldehyde. Vascular segments with one centimeter length were excised from the middle portion of each carotid artery, then subdivided into five segments with about 2mm length. All tissue sections were stained by Elastica Vangieson staining. The microscopic images of each transverse tissue section were digitized, and borders of vessel layers were manually traced, then intima to media area ratio (IMAR) was calculated using an image-processing software, NIH Image. The mean IMAR from five consecutive transverse tissue sections was used as the representative IMAR in each animal.

Data presentation and statistical analysis: All data were expressed as mean±SD, and analyzed by unpaired *t*-test. Because of limited number of the low dose group animals, *t*-test was used instead of one-way ANOVA. Difference was accepted as statistically significant when p value was less than 0.05.

Results

Effect of suramin on vascular smooth muscle cells: A10 cells were cultured in DMEM containing 0.5% FBS for 48 hours in order to synchronize the cell-cycle to G0/1 phase. Preliminary experiments revealed that complete removal of FBS rapidly decreased the cell viability (data not shown). Synchronized A10 cells were stimulated by either 10ng/ml PDGF-AB or 2% FBS in the presence of various concentrations of suramin (0 to 400μM) for 24 hours, then DNA synthesis was assessed by [^{3}H] -thymidine uptake. The DNA synthesis stimulated by 2% FBS was partially inhibited by high concentration of suramin. On the other hand, PDGF-AB stimulated DNA synthesis was inhibited by suramin significantly and dose dependently. The IC50 of suramin for PDGF-AB-stimulated DNA synthesis was 80μM from the dose-response experiments (Figure 1). The suramin's inhibitory effect for DNA synthesis had a strict correlation with the incubation time. Longer incubation with suramin resulted in more significant inhibition of DNA synthesis in A10 cells. The inhibition of DNA synthesis in the cells incubated with 100μM suramin for 90 minutes was about 60% of that observed in the cells exposed to suramin for 24 hours (Figure 2). The inhibitory effect of suramin on DNA synthesis had a linear correlation with the incubation time up to 90 minutes (Figure 2 inset). In order to investigate the isoform specificity of suramin's anti-PDGF activity, A10 cells were stimulated either by 2% FBS, 10ng/ml PDGF-AA, 10ng/ml PDGF-AB or 10ng/ml PDGF-BB for 24 hours with (or without) 100μM suramin. Among three PDGF isoforms, PDGF-BB provoked highest DNA synthesis in A10 cells, which was almost comparable to that induced by 2% FBS. On the contrary, the extent of PDGF-AA-stimulated DNA synthesis was very low in A10 cells.

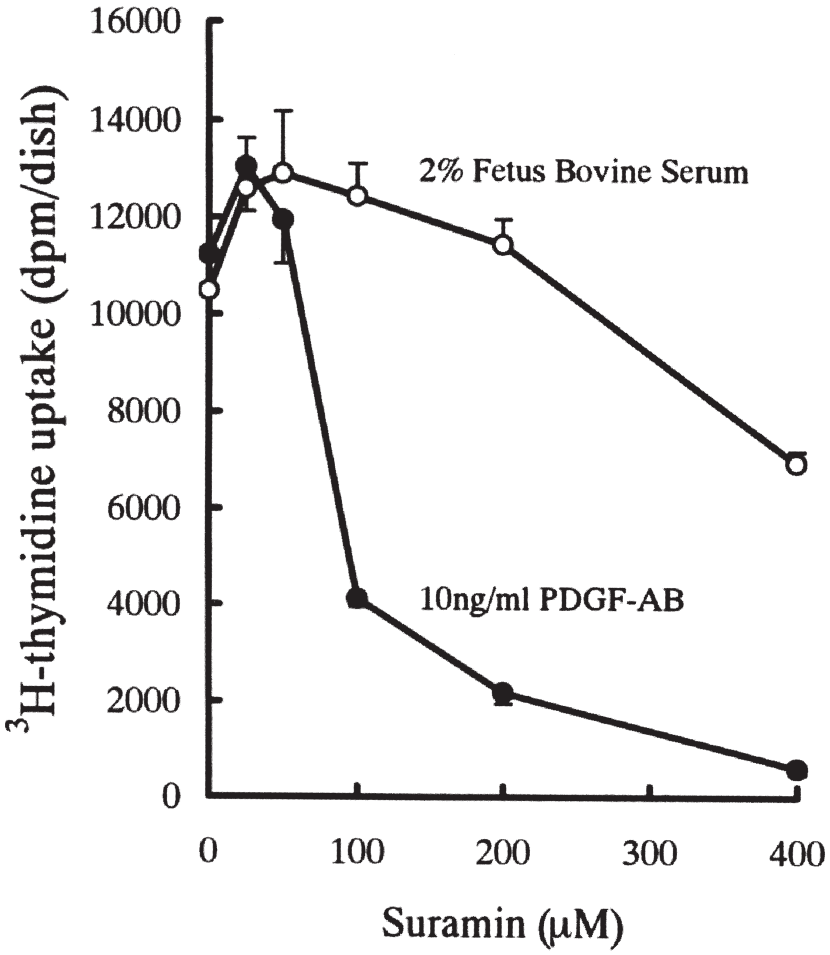

Figure 1 Effect of suramin on serum- or PDGF-stimulated DNA synthesis in A10 cells

A10 cells were synchronized to G0/1 by serum deprivation for 48 hours, then stimulated by Dulbecco's Modified Eagle Medium (DMEM) supplemented with 2% fetus bovine serum or DMEM containing 10ng/ml PDGF-AB for 24 hours in the presence of various concentrations of suramin. DNA-synthesis in A10 cells were assessed by ^{3}H -thymidine uptake. Each point represents the mean value of four different experiments.[84)]

Although the inhibition of DNA synthesis was statistically significant in all cases, suramin suppressed the PDGF-AB-induced DNA synthesis far more efficiently than those provoked by the other two PDGF isoforms (Figure 3). RVSMC were also arrested in G0/1 by serum deprivation for 24 hours, then stimulated either by 2% FBS or 10ng/ml PDGF isoforms for 24 hours in the presence (or absence) of 100mM suramin. PDGF-AA- and PDGF-AB-induced DNA synthesis were significantly inhibited by suramin. FBS-induced DNA synthesis of RVSMC was also suppressed

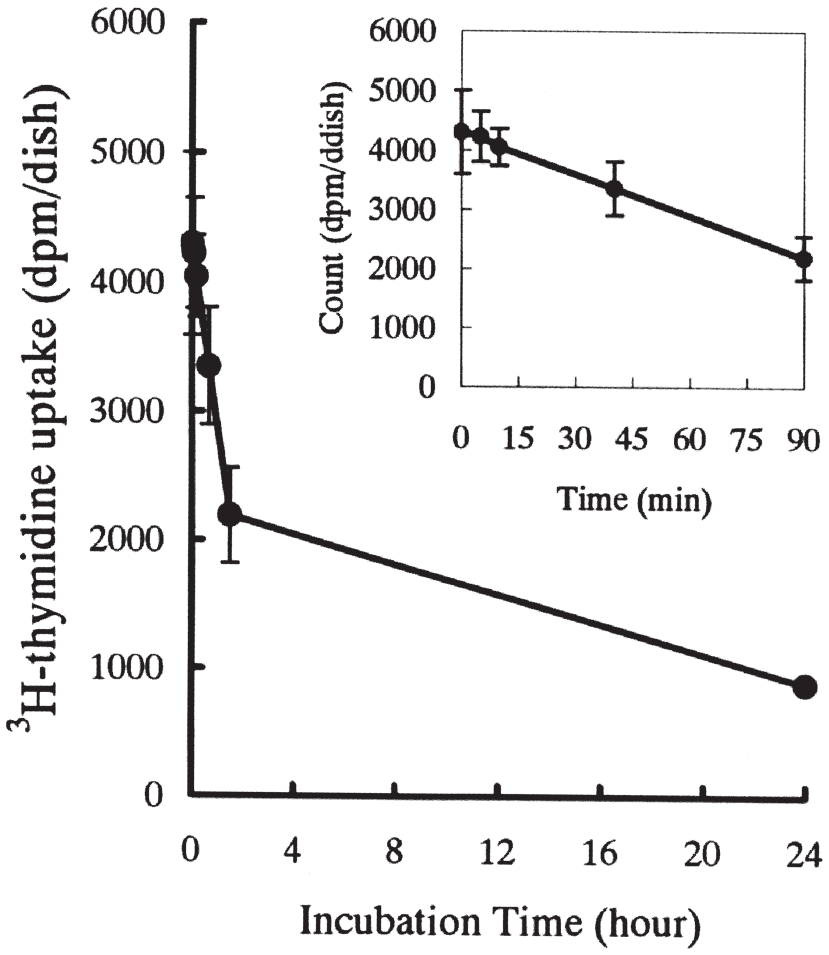

Figure 2 Time-dependency of suramin's inhibitory effect on PDGF-stimulated DNA synthesis in A10 cells
A10 cells were synchronized to G0/1 by serum deprivation for 48 hours, then stimulated by Dulbecco's Modified Eagle Medium (DMEM) containing 10ng/ml PDGF-AB and 100mM suramin for 24 hours. At indicated time points, medium was exchanged to DMEM containing PDGF-AB only, then incubation was carried out for the rest of the stimulation period. Duration of the stimulation period was adjusted to 24 hours in all conditions. DNA-synthesis in A10 cells were assessed by ^{3}H-thymidine uptake. The inset shows data at early time points. Each point represents the mean ± SD of four different experiments.[84]

by suramin (Figure 4).

Inhibition of intimal hyperplasia by suramin: Three weeks after the balloon-mediated vascular injury, common carotid arteries of control rabbits showed significant intimal hyperplasia, in which neointimal layer had almost comparable

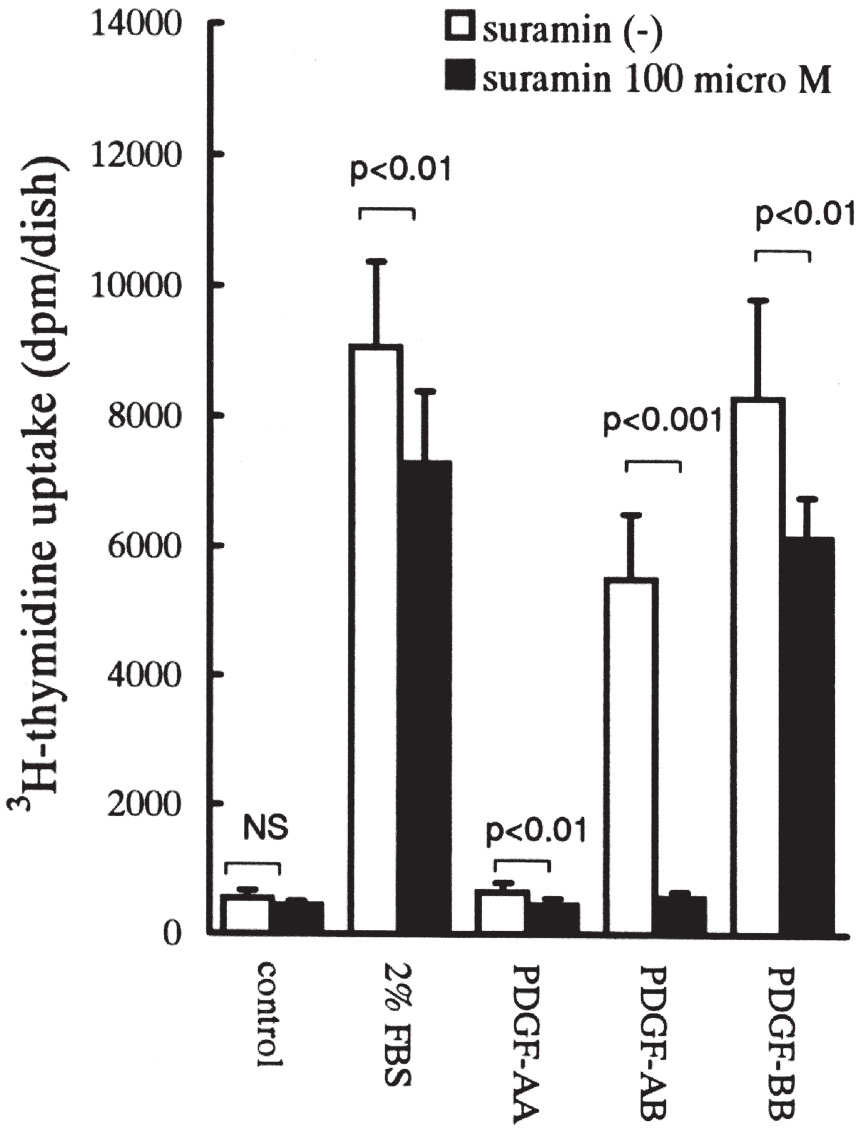

Figure 3 Suramin's inhibitory effect on DNA synthesis in A10 cells
A10 cells were synchronized to G0/1 by serum deprivation for 48 hours, then stimulated by Dulbecco's Modified Eagle Medium (DMEM) containing 2% fetus bovine serum, 10ng/ml PDGF-AA, 10ng/ml PDGF-AB or 10ng/ml PDGF-BB, respectively, for 24 hours with (or without) 100mM suramin. DNA-synthesis in A10 cells were assessed by ^{3}H -thymidine uptake. Each bar represents the mean+SD of eight different experiments.[84)]

thickness to that of medial layer. Histological examination revealed that one time local infusion of suramin significantly inhibited the neointimal formation at the site of vascular injury (Color fig. 14 and 15). Suramin dose dependently inhibited the

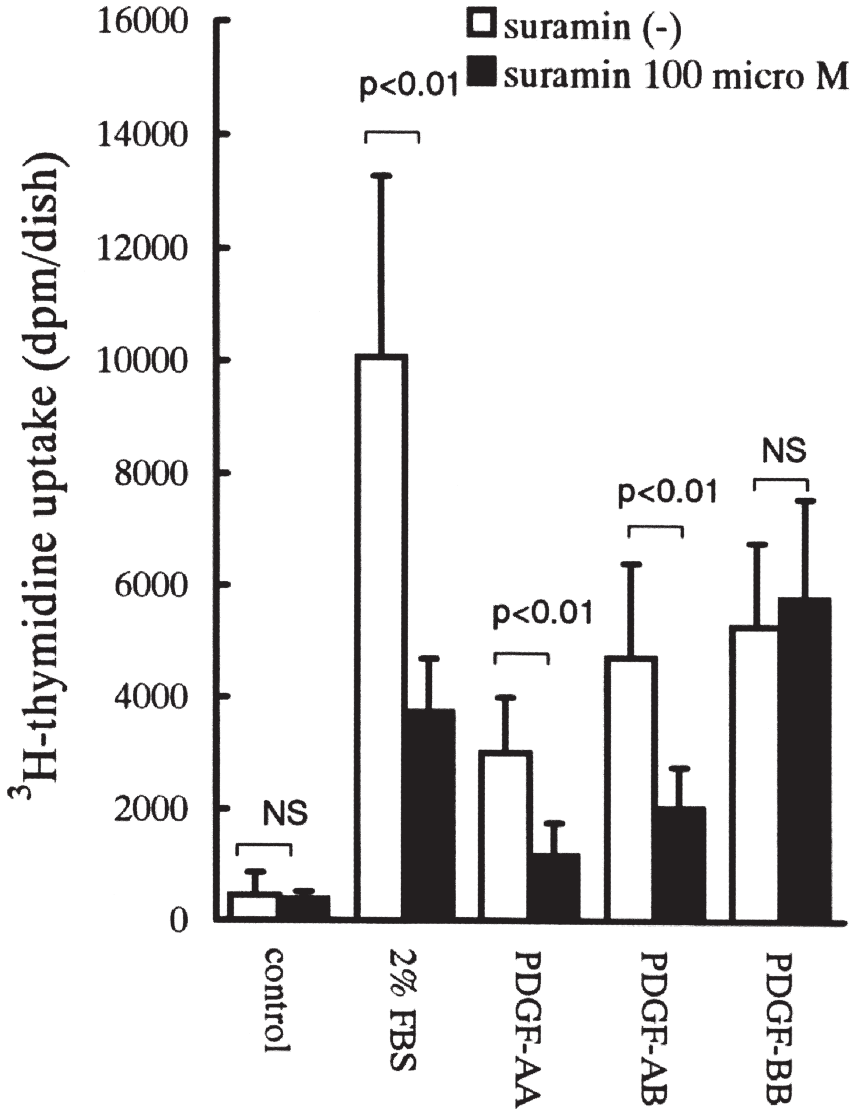

Figure 4 Suramin's inhibitory effect on DNA synthesis in the primary culture of rat vascular smooth muscle cells
Rat vascular smooth muscle cells obtained by explant method were synchronized to G0/1 by serum deprivation for 24 hours, then stimulated by Dulbecco's Modified Eagle Medium (DMEM) containing either 2% fetus bovine serum, 10ng/ml PDGF-AA, 10ng/ml PDGF-AB or 10ng/ml PDGF-BB for 24 hours with (or without) 100mM suramin. DNA-synthesis was assessed by ^{3}H-thymidine uptake. Each bar represents the mean+SD of eight different experiments.[84)]

neointimal formation after vascular injury, and the intima to media area ratios of control group, 0.5mM suramin group and 1.0mM suramin group were 48.8±14.9%, 21.0±12.0% and 12.2±6.0%, respectively ($p<0.05$ for control group vs. low dose

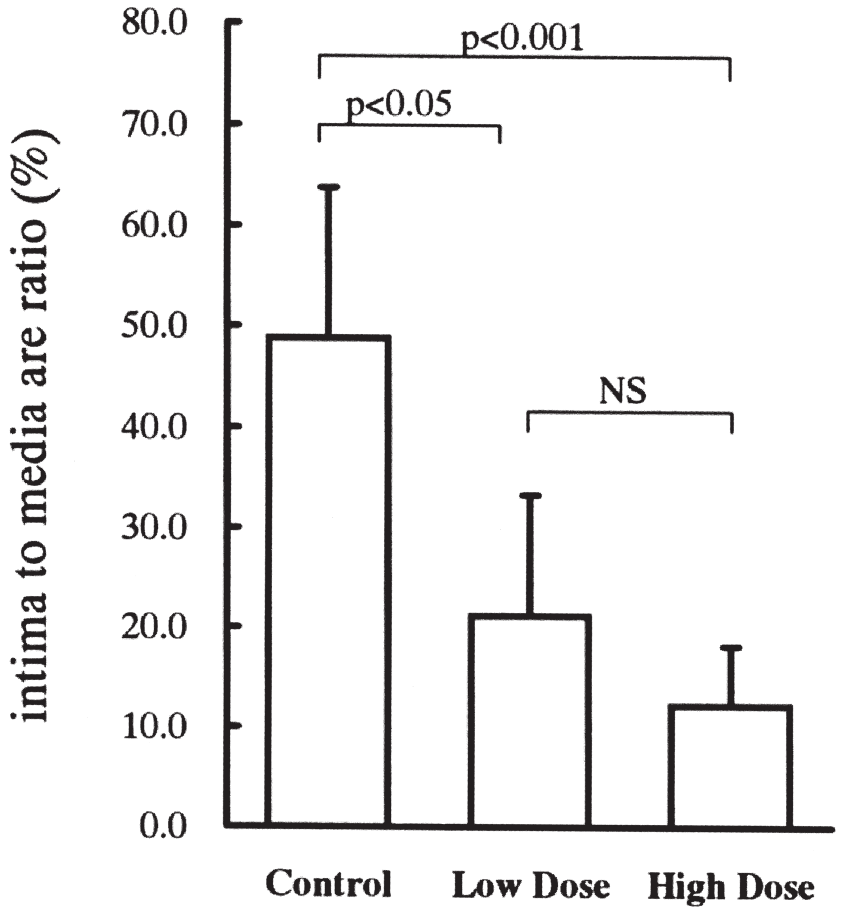

Figure 5 Quantitative analysis of the suramin-mediated suppression of intimal thickening after vascular injury
The photographs of tissue sections were digitized and the extent of neointimal formation was analyzed by using an image processing software. The intimal hyperplasia was expressed as the intima to media area ratio. Each bar represents the mean+SD of six (control and 1mM suramin group) or three (0.5mM suramin group) rabbits.[84]

group, $p<0.01$ for control group vs. high dose group) (Figure 5).

Discussion

Despite the rapid progress of the device technology in the field of coronary intervention, restenosis rate after catheter-based coronary angioplasty is still high. In fact, nearly 40% of the patients treated by balloon angioplasty alone have shown angiographical restenosis, and roughly half of them needs target lesion revascularization either by re-intervention or coronary artery bypass surgery[1]. To date, various pharmacological drugs such as anti-platelet drugs, Ca antagonist, angiotensin converting enzyme inhibitor, lipid lowering drugs and steroid have been used in

anticipation of their preventive effect against coronary restenosis[5)-10)]. Although most of these drugs suppressed SMC proliferation *in vitro* and some of them prevented intimal thickening after vascular injury *in vivo*, they have failed to show clinical benefit except for a few drugs[11)-13)]. Because previous investigations using the atherosclerotic plaques of human coronary arteries have shown that SMC and extracellular matrix were the major components of restenotic tissue, SMC proliferation should be the target to prevent coronary restenosis. Coronary restenosis is, however, a fairly complex biological process[3)]. A wide variety of growth factors and cytokines, such as PDGF, transforming growth factor β (TGFβ), epidermal growth factor (EGF), are responsible for the migration and proliferation of SMC[14)].

A polyanionic compound, suramin, was originally designed as a drug for trypanosomiasis and onchoceriasis[15)]. It is well known that suramin has a unique character as an anti-growth factor agent with broad spectrum. PDGF, EGF, TGFβ, basic fibroblast growth factor (bFGF), insulin-like growth factor and interleukin-6 (IL-6) are known to be inhibited by suramin[16)-20)]. Not only these growth factors and cytokines but also several key enzymes are suppressed by suramin. These include protein kinase C, phosphatidylinositol kinase, diacylglycerol kinase, DNA polymerase, DNA topoisomerase II, and reverse transcriptase[21)-25)]. These unique pharmacological properties might be the reason why suramin has shown antiproliferative effect on variety of human cancer cell lines, such as those obtained from rhabdomyosarcoma, multiple myeloma, prostate cancer and breast cancer[26-29]. As such, the pharmacological characteristics of suramin seem to be quite suitable for the prevention of SMC proliferation after vascular injury, a complex cellular response composed of receptor activation, intra-cellular signaling and DNA replication.

In this study, we examined the antiproliferative effect of suramin by utilizing two different experimental settings; (I) cultured vascular smooth muscle cells and (II) rabbit vascular injury model. PDGF-stimulated DNA synthesis of SMC was inhibited by suramin significantly and dose-dependently, and its IC50 was calculated to be 80μM (Figure 1). A previous report using radioactive PDGF ligands revealed that suramin's IC50 for the binding of PDGF with its receptor was 60μM, which is comparable to the value obtained in our experiments[30)]. Interestingly, weak growth stimulatory effect was observed at relatively low concentration (25μM) of suramin, though the increase of cellular DNA synthesis at this concentration was not statistically significant. Such pleiotropic action of suramin was also reported previously in an experiment using cancer cells[31)]. It was suggested that low concentration of suramin could release membrane-bound transforming growth factor a (TGFα) and increase its potential to activate cell surface epidermal growth factor receptor[32)]. Because of such pleiotropic action, it would be appropriate to maintain relatively high concentration of suramin at the site of action. The dose-response experiment suggested that higher local concentration of suramin could provide better antiproliferative effect when suramin was used *in vivo* situa-

tion. Although there are several reports suggesting non-specific cytotoxic effect of suramin, the structural features of A10 cells, such as cell size, cell shape and perinuclear structures, did not alter throughout the experiments even at the highest concentration of suramin (400μM) used in this study.

In order to assess the temporal profile of suramin's antiproliferative effect, A10 cells were incubated with 10ng/ml PDGF-AB and 100μM suramin for various time length. At the indicated time points, culture media were exchanged to those containing only PDGF-AB, and growth stimulation was continued for the rest of the incubation period. The entire stimulation period was adjusted to 24 hours in all conditions. As shown in Figure 2, the inhibition of PDGF-stimulated DNA synthesis was strictly dependent to the time length of incubation with suramin. Inhibition of DNA synthesis observed at 90 minutes exposure to suramin was 60% of that observed in the cells exposed to suramin for entire 24 hours. Interestingly, the anti-proliferative effect of suramin had a linear correlation with the incubation time up to 90 minutes (Figure 2 inset). This observation clearly suggested that longer exposure to suramin could provide more significant inhibition of the cellular DNA synthesis.

It was reported that suramin directly interacted with PDGF molecules since suramin inhibited the interaction between PDGF and anti-PDGF antibody[30]. In our experiments, suramin inhibited PDGF-AB - induced growth stimulation much more effectively than PDGF-BB - induced growth stimulation (Figure 3 and 4). These findings suggested that suramin might have a higher affinity to PDGF-A chain than to PDGF-B chain. It has been reported that established cell lines show different response to various physiological stimuli compared to primary culture cells, even though they were originated from the same tissue. Thus, we tested the effect of suramin using explanted rat aortic SMC (RVSMC). The DNA synthesis triggered by PDGF-AA and PDGF-AB was significantly inhibited by suramin in RVSMCs. On the other hand, PDGF-BB - stimulated DNA synthesis was not affected by suramin. These data also suggested that suramin had a preference to PDGF-A chain. In RVSMCs, PDGF-AA elicited more prominent response than A10 cells, which may suggest distinctive receptor subtype composition in each cell. Serum - induced DNA synthesis was suppressed by suramin more effectively in RVSMC than in A10 cells, indicating different serum-dependency of these cell lines.

Balloon-mediated removal of endothelial layer from rabbit carotid arteries promoted significant intimal thickening three weeks after the endodenudation procedure. Histological examination proved that neointima was composed of pure smooth muscle cells and that these rabbits were appropriate model of human coronary restenosis (Color Fig. 16a, 16b). In this study, a porous balloon catheter was used for the local delivery of suramin in order to maintain high local suramin concentration, and at the same time to reduce the total amount of suramin. Based on the findings obtained from *in vitro* experiments, we used 0.5mM and 1.0mM suramin solution and 10 minutes incubation time. Because blood flow was com-

pletely interrupted during balloon inflation, the local concentration of suramin was expected to be almost the same as that of the infused solution. As shown in Figure 5, neointimal formation after vascular injury was inhibited by suramin significantly and dose-dependently. The intima to media area ratio in high dose group was about 25% of that in control group. It was reported that intravenous injection of suramin attenuated the neointimal formation of rabbit abdominal aorta after the indwelling of polyethylene tubing for 24 hours[33]. Balloon-mediated endothelial denudation might be more appropriate mean to mimic the vascular injury caused by PTCA procedure. In addition, suramin was delivered using a local drug-delivery catheter in our study. Local drug delivery is advantageous to reduce the total amount of suramin, and at the same time, to maintain high local drug concentration at the target lesion. More recently, Gary *et al*. reported that chronic infusion of suramin inhibited the neointimal formation in rabbit iliac arteries after balloon injury[34]. It should be emphasized that, in our study, one time administration of suramin was shown to be sufficient to inhibit the neointimal formation after balloon injury.

Through many pharmacokinetic studies in human trypanosomiasis patients, it has been reported that suramin is tightly bound to plasma proteins (mostly serum albumin) and has a strikingly long elimination half-life, about 36 days[35]. Most common side effects of suramin were polyneuropathy, allergic skin rash and renal dysfunction. Rare side effects include agranulocytosis, hemolytic anemia and shock. Because most of these side effects were dose-dependent, local drug delivery regimen would be worthwhile to minimize the toxicity of this type of drug. Although in vivo localization of suramin is still controversial, based on the previous report, some part of locally delivered suramin might be accumulated in vascular endothelial cells and assumably underlying vascular smooth muscle cells[36].

In summary, an anti-growth factor agent, suramin, significantly inhibited the DNA synthesis in cultured vascular smooth muscle cells. Moreover, one time local infusion of suramin significantly suppressed the neointimal formation after vascular injury in an animal model. These results clearly suggested that pharmacological intervention targetting the growth factor's signaling pathway would be a promising and practical approach to prevent SMC proliferation.

3. Adenovirus-mediated Over-expression of a Cyclin-dependent Kinase Inhibitor p57Kip2 uppressed Vascular Smooth Muscle Cell Growth

In this study, we prepared three different replication-deficient adenovirus constructs expressing p21 family members, p21Waf1, p27Kip1 and p57Kip2, respectively, and investigated the effect of p57Kip2 and two other CKI on the proliferation of cultured vascular smooth muscle cells and the neointimal formation in an animal model.

Materials and Methods

Animals: Male Japanese White rabbits (body weight 2 to 2.5 kg) were maintained on a normal chow diet. Anesthesia was induced using pentobarbital sodium injection (50 mg/kg body weight).

Preparation of Adenovirus Constructs: A cosmid vector with CAG promoter, pAdexCA1w, was used in this study. In order to make replication-deficient adenovirus constructs expressing CKIs, COS-TPC method was used as described previously[37]. First, mouse p27Kip1 and p57Kip2 cDNA were ligated with pAdexCA1w, then these cosmids were cotransfected into 293 cells with the partially digested parental adenovirus DNA. Homologous DNA recombination between cosmids and adenovirus DNA within the 293 cells provide adenovirus constructs. In order to enable the detection of CKI protein expression, the nucleotide sequence encoding α-Flag was fused in-frame to 5' end of the p27Kip1 and p57Kip2 cDNA, respectively. The resultant recombinant adenovirus constructs, designated as Adex-p27 and Adex-p57, were purified by CsCl2 gradient ultracentrifugation followed by extensive dialysis. Adex-p21 was generously gifted by Dr. Ueno (Kyushu University, Japan). The titer of each adenovirus stock was assessed by a plaque-formation assay using the 293 cell. A control adenovirus, Adex-LacZ expressing bacterial β-galactosidase, was prepared in the same way.

Cell Culture: (refer to the method sectopn of II)

Western Blot Analysis: A10 cells infected either with Adex-p21, Adex-p27 or Adex-p57 were treated with lysis buffer (**STEP buffer**, 1% Triton-X, 1% SDS) and subjected to 12% sodium dodecil sulfate - polyacrylamide gel electrophoresis (SDS-PAGE), then electrically transferred onto nitrocellulose membranes. The membrane was probed with a mouse monoclonal antibody against human p21Cip1 (6B6, Pharmingen, San Diego, CA) and a mouse monoclonal antibody against α-Flag (Anti-FLAG M5, Eastman KODAK, USA) then visualized by using an alkaline phosphatase-conjugated anti-mouse IgG and chromogenic reagents (AP Conjugate Substrate Kit, BIO-RAD, USA).

FACS Analysis: Quiescent A10 cells were prepared by 48 hours serum deprivation. The quiescent cells were infected with 30 moi of Ad-CKIs (Ad-p21, Ad-p27, Ad-p57) and then stimulated by exposing to the culture medium containing 10% FBS. Control cells were infected with 30 moi of Ad-LacZ. These cells were stained by propidium iodido, then analyzed by a **COULTER FACScan and EXPO Cytometer software**.

Measurement of DNA Synthesis: Effect of Ad-CKIs on cellular DNA synthesis was assessed by ^{3}H thymidine uptake. In detail, confluent A10 cells in 24-well plates were infected with either Ad-LacZ, Ad-p21, Ad-p27 or Ad-p57 at various moi for 1 hour or left uninfected, and incubated in serum-free medium for 24 hours. Culture medium was exchanged to the one containing 10% FBS, and culture was continued additional 24 hours. The cells were, then, pulsed for 1 hour with 1 μCi/ml of [^{3}H] -thymidine (DuPond NEN, USA). The incorporation of [^{3}H] -thymidine into

the trichloroacetic acid-insoluble fraction was measured using a scintillation counter.

In Vivo Gene Transfer into Rabbit Carotid Arteries: Carotid arteries of male Japanese White Rabbits were balloon-injured three times using a coronary angioplasty catheter (ENDURA, 3.0 mm diameter, 10 mm length; ACS, USA). After balloon-injury, an isolated space was created by clipping the distal end of common carotid artery and inflated balloon at the proximal end of common carotid artery. Adenovirus in PBS (1.0×10^9 pfu) was injected into the isolated space through the guide wire lumen of the balloon catheter. After 20 minutes incubation, the adenovirus containing solution was retrieved and blood circulation was restored by releasing the distal clipping and retrieving the proximal balloon catheter. The vessels were harvested 3 weeks later, perfusion-fixed in 10% paraformaldehyde, and tissue sections with Masson staining were prepared for microscopic examination. The cross-sectional areas of neointima and media were obtained by manual tracing of the boundaries of each vessel layer and an image analyzing software (NIH image).

CDK activity inhibited by p57Kip2: Serum-starved SMCs(A10) were infected with 30pfu/cell of either Adex-LacZ or Adex-p57 and then serum-stimulated with 10% FBS for 0h, 4h, 8h, 12h, 16h, 20h, 24h, 36h. Each of 30μg of protein lysis were applied to 6%SDS. on cellulose membrane over

PCR analysis of adenovirus gene sequences in various rabbit tissues: Three days after gene transfer procedure using Ad-LacZ, DNA was extracted from various rabbit tissues including kidney, brain, heart, testis, lung, smooth muscle, spleen, liver, blood, and carotid artery that was directly exposed to the adenovirus. The partial DNA sequence of adenovirus genom was amplified by using specific primers against adenovirus (sense primer; 5'-GGCAACGTG-CTGGTTGTTGT-3', antisense primer; 5'-ACCTTCTGATAGGCA GCCTG-3'). PCR products were analyzed through 1% agarose gel electrophoresis.

Data presentation and statistical analysis: All data were expressed as mean$\pm$SD, and analyzed by unpaired t-test. Difference was accepted as statistically significant when p value was less than 0.05.

Results

Adenovirus-mediated overexpression of CKIs in vascular smooth muscle cells: In order to compare the anti-proliferate effect of p21 family members, we prepared three different replication-deficient adenovirus constructs containing the entire coding sequence of CKI gene (p21Waf1, p27Kip1 and p57Kip2) and designated them as Ad-p21, Ad-p27 and Ad-p57, respectively. A10 cells were infected with 10 moi of Ad-p21, Ad-p27 or Ad-p57, and the protein expression of each CKI was evaluated by Western blot analysis three days after infection. As shown in Figure 6, A10 cells infected by each Ad-CKI expressed excess amount of CKI proteins with appropriate molecular weight, respectively.

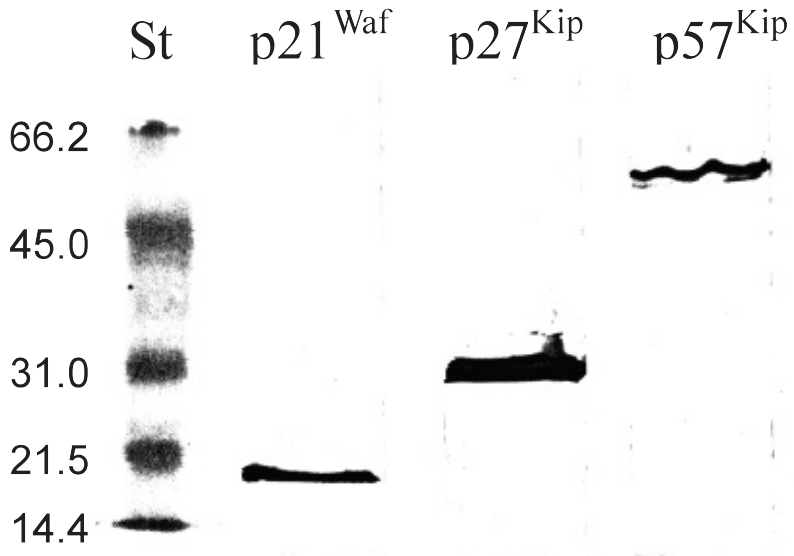

Figure 6 Expression of CDK inhibitors (p21Waf1, p27Kip1, p57Kip2) in vascular smooth muscle cells (A10 cells) infected with Ad-CKIs

Vascular smooth muscle cells (A10 cells) were infected with Ad-CKIs (10 moi). Three days later, ten micro grams of total cell lysates were subjected to SDS-PAGE and CKI proteins were detected on Western blot analysis using specific antibodies against each CKI.

We next tested the effects of CKI overexpression on serum-stimulated DNA synthesis. A10 cells were made quiescent by serum deprivation for 48 hours. This treatment reproducibly arrested nearly 90% of the cells in G0/G1 phases of the cell cycle as assayed by flow cytometry. The quiescent A10 cells were incubated with various amounts of Ad-CKI for 12 hours, then re-stimulated by exchanging the culture medium to that containing 10% FBS for additional 24 hours. Control cells were infected with 100 moi of adenovirus containing bacterial Lac Z gene (Ad-LacZ). Ad-CKI infection significantly suppressed the serum-induced DNA synthesis as measured by ^{3}H-thymidine uptake. Among three CKIs we tested, p57Kip2 showed the most significant suppression of cellular DNA synthesis (Figure 7). Flow cytometric analysis revealed that Ad-CKI infection induced marked G1 arrest in A10 cells (data not shown).

To test whether forced p57Kip2 expression affects the expression level of other p21 family members and phosphorylation level of Rb class pocket proteins, we harvested A10 cells every 8 hours after serum stimulation and performed Western blot analysis. In Ad-LacZ infected A10 cells, serum stimulation provoked the protein degradation of p27Kip1, and resulting in the increase of phosphorylated p107 and p130. All these serum-induced alterations were completely abolished by Ad-p57 infection (Figure 8).

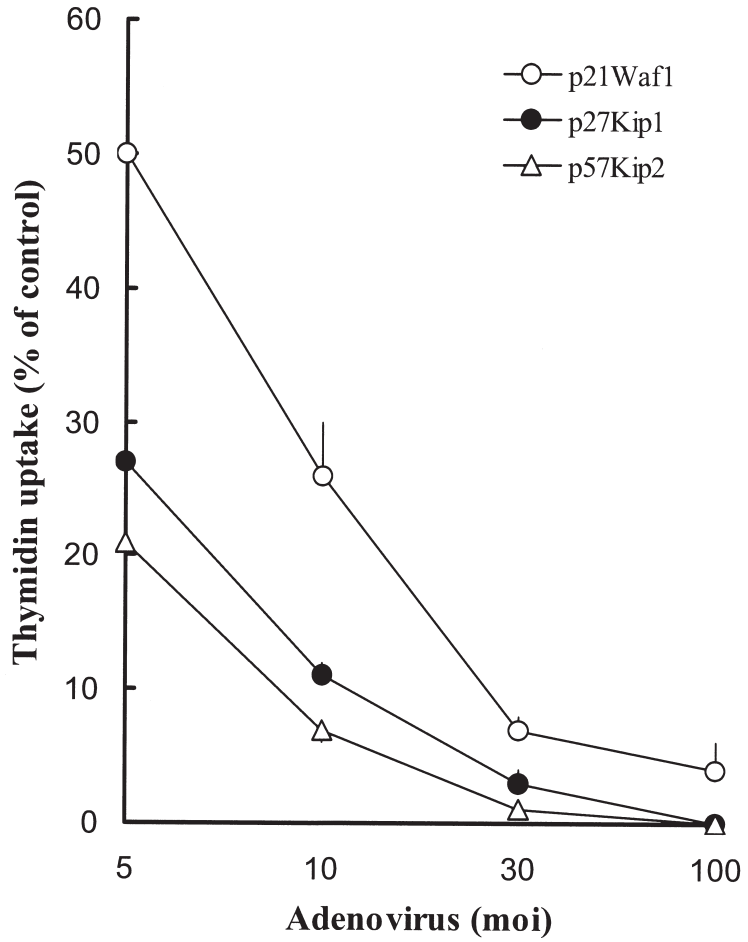

Figure 7 Effect of CKI on serum-stimulated DNA Synthesis of vascular smooth muscle cells
A10 cells were infected with the indicated amount of Ad-CKI. After 24 hours of serum deprivation, cells were stimulated with 10% FBS for following 24 hours, then pulse labeled by [^{3}H] -thymidine. Incorporated [^{3}H] -thymidine was extracted and measured by liquid scintillation counter. All data were normalized by the thymidine uptake in the Ad-LacZ infected A10 cells. Data were expressed as mean±SD (n=4).

Over-expression of CKIs inhibited neointimal hyperplasia in the rabbit carotid artery after vascular injury: We next tested whether local expression of p57Kip2 in arterial wall would efficiently suppress neointimal formation after vascular injury. Balloon injury model of rabbit carotid artery represents a well-characterized and highly reproducible model for vascular proliferative disorder. Preliminary experiments indicated that three times passage of inflated balloon successfully and reproducibly created massive proliferation of smooth muscle cells

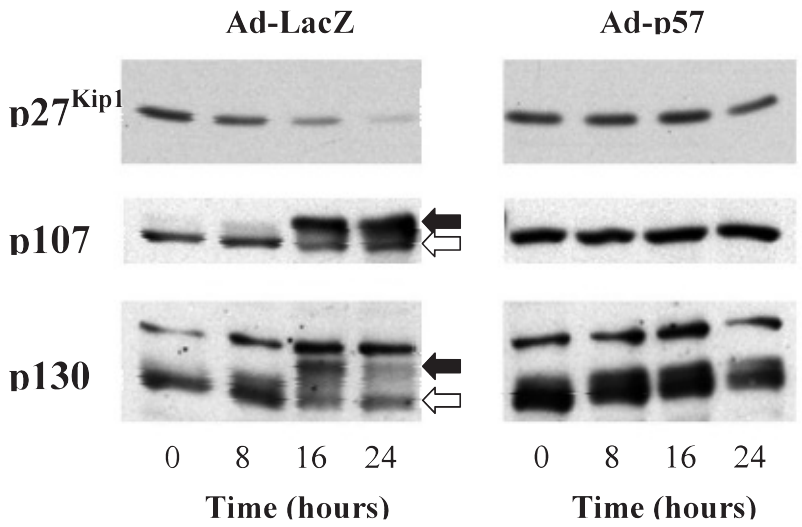

Figure 8 Effect of p57Kip2 expression on serum-induced degradation of p27Kip1 and phosphorylation level of pocket proteins, p107 and p130

A10 cells were infected with 30moi of Ad-p57. After 48 hours of serum deprivation, cells were stimulated with 10% FBS. Total cellular lysates were prepared at the indicated time point (0, 8, 16, 24 hours after serum stimulation). Twenty micro grams of protein lysates were subjected to SDS-PAGE and subsequent Western blot analysis using specific antibodies. White arrow: non-phosphorylated protein. Black arrow; phosphorylated protein.

resulting in thick neointimal formation. To assess the effects of p57Kip2 overexpression on the neointimal formation in this model, the balloon injured rabbit carotid arteries were infected with $1x10^9$ PFU of either Ad-p57 or Ad-LacZ. Arteries were harvested 3 weeks after balloon injury and the intima to media area ratio was assessed by using an image analyzing software. A marked reduction in neointimal formation was achieved by adenovirus-mediated overexpression of p57Kip2 (Color Fig. 11). Intima to media ratio from multiple experiments suggested that the antiproliferative effect of Ad-p57 was statistically significant (Figure 9).

Discussion

In this study, we utilized replication-deficient adenovirus vectors to introduce cyclin-dependent kinase inhibitor genes into cultured VSMC (A10 cells) and rabbit carotid arteries. Western blot analysis using specific antibodies revealed markedly enhanced expression of CKI in A10 cells after the infection of each adenovirus vector. All of the p21 family members significantly suppressed the serum-induced DNA synthesis of A10 cells. Extent of the inhibitory effect was dependent to the amount of virus particles used for the infection. Since nearly 100% of gene transfer

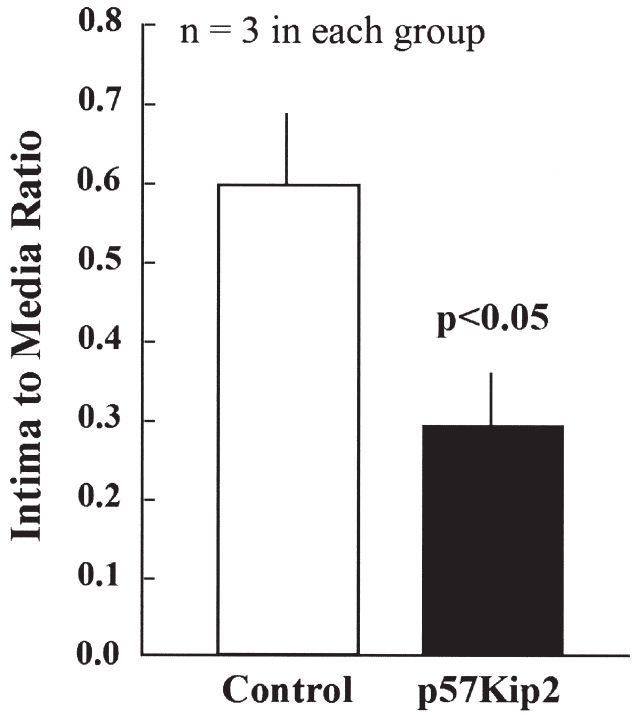

Figure 9 Quantitative Analysis of Neointimal Formation

Three weeks after balloon injury and adenoviral infection (1.0×10^9 pfu, Ad-LacZ or Ad-p57), right common carotid arteries were excised and tissue sections were prepared by Masson staining. Cross-section of carotid arteries were digitized, then the area of intima and media were quantited using image-processing software, NIH image (n=3).

efficiency was obtained by as low as 10 moi of Ad-LacZ, these results suggested that there might be a dose dependency between the extent of CKI protein expression and the inhibition of DNA synthesis. Among three CKI we tested, p57Kip2 showed the highest inhibitory effect on the cellular DNA synthesis especially at low virus doses.

Adenovirus-mediated p57Kip2 overexpression completely abolished the protein degradation of p27Kip1. Previous report suggested that p27Kip1 was removed from nucleus, transferred to proteosome, then degrade through Jab1-dependent mechanism. Because GST-pull down assay using GST-p57Kip2 protein indicated that p57Kip2 did not bind to Jab1 (data not shown), competitive inhibition of over expressed p57Kip2 and intrinsic Jab1 resulting in the increase of free p27Kip1 is unlikely. Results obtained in our study suggested p57Kip2 is located upstream of p27Kip1, and proceeding reduction of p57Kip2 is necessary for the degradation of

p27Kip1.

Rabbit carotid artery restenosis model was used in this study to test *in vivo* effect of p57Kip2 overexpression on the neointimal formation after vascular injury. In order to minimize the systemic side effect of adenovirus vectors, adenovirus were delivered locally to the closed short segment of the rabbit carotid artery which was created by a distal clump and inflated balloon positioned proximally, and retrieved as much as possible after 20 minutes of incubation period. Preliminary experiment using Ad-LacZ showed that the length of incubation time and the amount of adenovirus particle used in this study were enough to achieve effective gene transfer and subsequent protein production. One time local administration of Ad-p57 significantly inhibited the neointimal hyperplasia which was created by balloon-mediated endodenudation.

Expression pattern of cell cycle regulatory gene after vascular injury was reported by Tanner et al[38), 39)] Protein level of p27Kip1 was maintained at high level in uninjured rat carotid arteries, and fell rapidly within 48 hours after vascular injury. Two weeks after the injury, p27Kip1 protein expression was gradually returned to control level. On the contrary, p21Waf1 protein level is kept low in normal arteries and increased in neointima after 7 days from vascular injury. From these results, it was concluded that reduction of p27Kip1 expression may trigger the cell cycle of VSMC and the accelerated expression of p21Waf1 at later time point may contribute to the re-establishment of the quiescent phenotype of VSMC after vascular injury[40)]. In contrast to the ubiquitous expression of p21Waf1 and p27Kip1, p57Kip2 is expressed in the tissues which are composed of terminally differentiated cells, suggesting that p57Kip2 is involved in a genetic program to exit cell cycle during differentiation[41), 42)]. Furthermore, only p57Kip2 knock-out mice were embryonic lethal while p21Waf1 and p27Kip1 knock-out mice were well survived[42)–44)]. These observations suggested that p57Kip2 has a key role during the development of embryo that can not be compensated by other CKI family members.

In order to obtain sufficient therapeutic effect and minimal side effect, it might be necessary to full-fill two opposite goals; high viral concentration at the site of action and very low (or no, if possible) viral escape to the systemic circulation. Thus, catheter-based local delivery system was utilized in this study. Injured vascular wall was exposed to adenovirus particles only for 20 minutes within a closed vascular segment, and virus solution was retrieved as much as possible through drug-delivery balloon catheter. PCR analysis, however, demonstrated that adenovirus genome was extracted not only from carotid arterial wall, but also from liver, spleen and heart (data not shown). From the experiments using contrast medium, relatively large amount of medium was leaking out from the closed vascular segment to the systemic circulation via vasa vasorum. These results suggest that tissue-specific promoter / enhance sequence might be necessary to be implemented into the adenovirus vector for tissue-specific gene expression.

In summary, the present study clearly suggests that p57Kip2 is a potent negative regulator of VSMC growth both in vitro and in vivo. Although there is little evidence which cyclin/CDK complex is the specific target of p57Kip2, the expression studies reported here demonstrated that p57Kip2 might be playing a pivotal role in cell cycle progression, especially early phase of G1-S transition of VSMC. Further elucidation of the precise role of p57Kip2 in cell cycle might provide us better understanding of molecular pathology of coronary restenosis, and ultimately lead to a new gene therapy to treat various vascular proliferative disorders.

4. Coordinated downregulation of p57kip2 and p27kip1 are involved in vascular smooth muscle cell (VSMC) proliferation.

G1 progression of the cell cycle and entry into S phase require the binding and activation of cyclin/CDK complexes, such as cyclin-D/CDK4, cyclin-D/CDK6 and cyclin-E/CDK2 holoenzymes[45), 46)]. The CDK inhibitor (CKI) can inhibit cyclin/CDK activity and subsequent phosphorylation of Rb, resulting in G1 arrest[47), 48)]. The CKI consists of two protein families; INK4 family ($p15^{INK4b}$, $p16^{INK4a}$, $p18^{INK4c}$, $p19^{INK4d}$), which appear to specifically target D type-cyclin kinases49, and p21 family (p21Cip1, p27Kip1, p57Kip2), broader inhibitors for all G1 cyclin /CDK complexes[50)]. It has been shown that overexpression of each p21 family can induce cell cycle arrest at G1 phase[51)].

In vivo experiments have shown that both p27Kip1 and p21Cip1 exert distinct roles respectively in SMC proliferation after arterial injury[52), 53)]. While distribution of p21Cip1 and p27Kip1 is quite ubiquitous[54)], p57Kip2 mRNA is expressed in only terminally differentiated tissues, including heart and skeletal muscle[55), 56)]. Forced expression of p57Kip2 in proliferating skeletal muscle myoblasts can trigger not only G1/S phase block by inhibiting cyclin/CDK complexes but also stabilize MyoD, a strong basic helix-loop-helix (bHLH) type transcriptional factor, via direct binding[57), 58)]. Thus, p57Kip2 may function in myogenic differentiation by at least two distinct mechanisms. An attractive scenario is that these two different function of p57Kip2 might confer myogenic differentiation on skeletal muscle cells, and similar mechanisms are functioning in the SMC differentiation. To date, the functional role of p57Kip2 during the proliferation of immature SMC has remained unknown.

In this study, we investigated the role of p57Kip2 and the kinetics of G1 phase cell cycle related proteins during SMC proliferation.

Materials and Methods

Preparation of anti-p57kip2 polyclonal antibody: Polyclonal antibodies against p57Kip2 C-terminal was prepared by injecting 500μg GST-p57 fusion protein intradermally into rabbits at biweekly. Rabbit polyclonal antibody was purified as described by Ed Harlow[59)]. Antibody specificity for p57Kip2 was certified by the

westernblot using the lysate of p57Kip2 overexpressing A10 cells.

Cell culture and synchronization: (refer to the method section of II)

Cell cycle analysis by flow cytometer: Ethanol fixed cells were stained by addition of 700μl of 20μg/ml propidium iodide for 30 minutes. The fluorescence of DNA was measured using a flow cytometer (FACSCalibur, Becton Dickinson), and the cell cycle distribution was analysed by using a computer software (Cell Quest / ModFit LT, Becton Dickinson).

Reverse Transcription (RT) and Polymerase Chain Reaction (PCR) for quatificaiton of p21Cip1, p27Kip1, p57Kip2, SM1/2, SMemb and GAPDH mRNA: Total RNAs (1μg) were reverse transcribed to cDNA, and amplified by thermal cycler. Based on the GeneBank database, PCR primer sequences were desinged;

rat p21Cip1		
	sense	5'-ATG-TCC-GAT-CCT-GGT-GAT-GT-3'
	antisense	5'-GGC-GCT-TGG-AGT-GAT-AGA-AA-3'
rat p27Kip1		
	sense	5'-AAC-GTG-AGA-GTG-TCT-AAC-GGG-AG-3'
	antisense	5'-TGC-GAA-GAA-GAA-TCT-TCT-GCC-GCA-3'
mouce p57Kip2		
	sense	5'-TGA-CCT-CAG-ACC-CAA-TTC-CG-3'
	antisense	5'-TTC-GAC-GCC-TTG-TTC-TCC-TG-3'
rat SM1／2		
	sense	5'-ATG-AGG-CCA-CGG-AGA-GCA-ACG-A-3'
	antisense	5'-CCA-TTG-AAG-TCT-GCG-TCT-CGA-3'
rat SM emb		
	sense	5'-ATG-GGA-AGA-AGG-TGA-AGG-TGA-AC-3'
	antisense	5'-TGG-ACA-GGA-AGC-GGT-ATT-TAT-TG-3'
rat GAPDH		
	sense	5'-GCT-GCC-TTC-TCT-TGT-GAC-AAA-3'
	antisense	5'-CAC-GCC-ACA-GCT-TTC-CAG-A-3'

Amplified DNAs were resolved by agarose gel electrophoresis and visulalized by ethidium bromide staining. In a preliminary experiments, all products were verified by sequencing and confirmed to be the target cDNA (Data not shown). To ensure that quantification took place in the exponential phase of PCR, the fluorescence intensities of DNA bands obtained at every two PCR cycles were plotted onto logarithmic graphs and the cycle numbers were determined at which all plotts were within a linear range.

Westernblot and immunoprecipitation: Ten mg (or 100μg for Rb family) of cellular proteins were resolved by SDS-PAGE (6-12%), transferred onto nitrocellulose membranes (Bio-Rad), blocked with 10% nonfat dry milk, and incubated with the primary antibodies. The membrans were incubated with HRP-conjugated secondary antibodies, and protein bands were visualized using ECL westernblot kit. Immuno-precipitations were performed by incubating 500μg of total cell lysate with

5μg of anti-cyclin antibodies after preclearing with normal rabit and mouce IgG. To precipitate immune complexes, protein A/G Sepharose beads (30μl of 50% slurry) was added and genlty rotated for overnight, then precipitates were washed four times in lysis buffer and used for westernblot analysis.

Kinase Assay of immunoprecipitated cyclin/CDK complex: Cells were scraped and suspended in ice-cold kinase lysis buffer (refer to the method sectoion of III). Total lysates were sonicated and pre-cleared with normal rabbit and mouce IgG-coated protein A/G beads for one hour. Cleared supernatants were precipitated with protein A/G sepharose beads precoated with saturating amount of each antibody for 2 hours at 4°C. Beads were washed 4 times with kinase lysis buffer and once with HEPES buffer (50mmol/L HEPES-pH7.5, 1mmol/L DTT). The pellets were resuspended in 5μl of reaction buffer (200mmol/L Tris-HCl pH7.4, 100mmol/L MgCl2, 45mmol/L β-mercaptoethanol, 10mmol/L EGTA, 1mmol/L DTT, xxx mol/L [γ-^{32}P] ATP) containing either 1μg of GST-Rb protein (cyclin-D associated kinases) or 5mg of Histone H1 (cyclin-E associated kinase), and incubated for 30 minutes at 30°C. The kinase reaction were stopped by adding SDS sample buffer and boiling for 5minutes. Labeled proteins were resolved on 10% SDS-PAGE and subjected to autoradiography.

Construction and transfection of adenoviruses: (refer to the method section of III)

Transient transfection and flow cytometry analysis: Full-length p57Kip2 cDNA was subcloned into mammalian expressing vector, pcDNA3 (Invitrogen). Subconfluent A10 cells in 150 mm culture dish were transfected with calcium-phosphate precipitates of 23μg plasmid DNA. Six hours later, precipitates were removed and cells were cultured in fresh medium for 48 hours thereafter. The cells were rinsed off the plates with PBS containing 0.1% EDTA, pelleted, and stained with FITC-conjugated anti-CD20 antibody (Becton Dickinson). Subsequently, cells were fixed with 70% ethanol for 30 minutes and stained with propidium iodine as stated before. Flow cytometric analysis was performed and CD20-positive cells were selected by gating at the range where vacant vector transfected cells were definitely negative. The propidium iodide signal was used to measure cellular DNA content.

Results

Time course of cell cycle: First, we evaluated the time course of cell cycle. After 60 hours serum starvation, more than 90% of A10 cells were synchronized at G0 arrested phase (Figure 10A, B, C). Progression of cell cycle from G1 to S phase started at about 10 hours after serum stimulation and S phase peak was observed at 16 hours. After completion of S phase progression, G2/M phase entry began at about 18 hours. One round of cell cycle seemed to be completed by 24 hours and second cycle of G1 phase was ongoing from 24 hours to 36. Therefore, we evaluated expresson kinetics of cell-cycle related proteins up to 20 hours after serum stimulation in the following experiments.

Phenotypic alteration after serum starvation and during proliferation: The A10

A

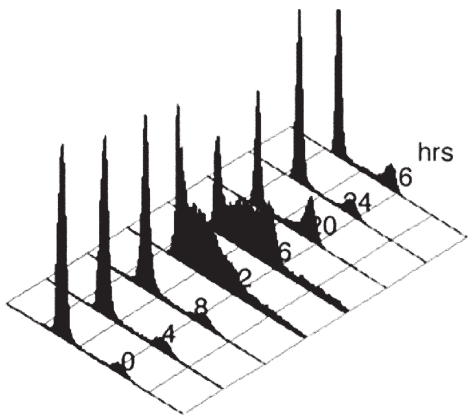

B

serum (h)	0	4	8	12	16	20	24	36
G0/G1(%)	91.7	92.1	93.7	47.8	16.2	65.0	88.5	79.3
S(%)	5.3	3.5	2.8	66.8	73.8	12.3	6.0	11.0
G2/M(%)	3.0	3.4	3.5	4.0	4.4	22.7	5.5	9.6

C

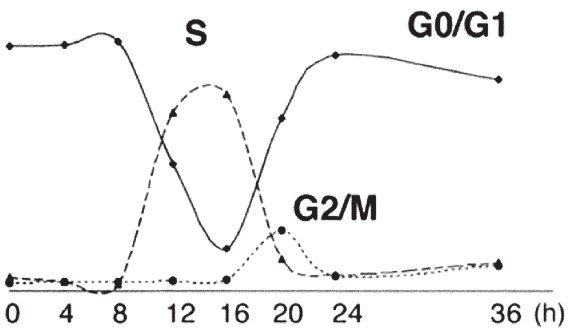

Figure 10 Cell cycle distribution after serum stimulation
A, G0 arrested A10 cells were stimulated with growth medium. At indicated time point, cells were harvested, stained with propidium iodine, and DNA contents were measured by flowcytometry. Representative raw data were shown. B, C, Mean values of three independent experiments.

cell line is derived from embryonic rat thoracic aorta[60] and widely used for many biological studies as proliferating SMC[61)-63)] Reportedly, they bear phenotypic similalities with immature SMC, which proliferate in neointima after coronary interventions[64)] We clarified whether immature A10 cells could differentiate to mature, contractile phenotype after serum deprivation. The smooth muscle myosin heavy chain (SM-MHC) isoform (SM1 and SM2) and non-muscle myosin heavy chain (NM-MHC; SMemb) have been used as important molecular markers of SMC differentiation status[65), 66)] The mRNA of SM1 and SM2 can be amplified

simultaneously by single pair of primers, because they are produced by alternative splicing from a single gene[67] PCR cycle numbers were determined so as to obtain linearity on the RT-PCR of these target mRNA, and used for the following examinations (data not shown). As shown in Figure 1A, mRNA of SM1 and SM2 were amplified together with this set of primers from rat heart total RNA. During cell proliferation, however, only SM1 mRNA was detected from A10 total RNA. Serum stimulation gradually decreased mRNA expression of SM1 as cell cycle progressed from G1 into S phase (Figure 11A, B, C). In the same way, mRNA of SMemb, a molecular marker for the embryonic phenotype of SMC[68), 69)], was expressed highly in G0 arrested A10 and was reduced after mitogenic stimulation. But both mRNAs of SM1 and SMemb were increased as S-phase was promoted. Even after serum starvation, A10 cells didn't exhibit mRNA of SM2, a molecular marker for the metured phenotype. In addition, mitogenic stimulation didn't alter their phenotypes except for a subtle change in the expression level of embryonic molecular genes.

mRNA and protein expressions of p21 family: To clarify which member of p21 family proteins are involved in the proliferative process after mitogenic stimulation, we examined the mRNA and protein expressions of p21 family proteins by quantitative RT-PCRs and westernblot analysis. As shown in Figure 12A, mRNAs of p21Cip1 and p57Kip2 were constantly expressed throughout the cell cycle. On the contrary, level of p27 mRNA significantly decreased after serum stimulation and re-accumulated during S phase. In consistent with the result of RT-PCR, protein expression of p21Cip1 was almost unaltered, but those of p27Kip1 and p57Kip2 abundantly expressed in G0 arrested cells, were decreased to 39% and 32% respectively soon after stimulation and bottomed out during S phase. Therefore, transcriptional regulation seems to play a critical role in the content of p27Kip1, though p57Kip2 is regulated mainly post-transcri-ptionally.

G1 cyclins and CDK protein expression: Figure 13 shows the protein expression of G1 phase cyclins and CDKs after serum stimulation. CDK4, CDK6 and cyclin-D3 levels were essentially invariable throughout the cell cycle. In marked contrast, transient upregulation of cyclin-D1 and -D2 were observed at G1 phase, though cyclin-E was expressed relatively low at G0 and early G1 phase. Cyclin-E started to accumulate at late G1 phase (later than cyclin-D1 and -D2 increase) and this elevation was maintained throughout S phase. CDK2 upregulation was shown at 16 hours and seemed to be preceded by the increase of cyclin-E level. Thus, among G1 cyclins and CDKs, accumulated protein levels were disclosed in cyclin-D1,D2 at G1 phase transiently and cyclin-E at late G1 phase, followed by CDK2 upregulation at S phase.

Cyclin/CDK enzymatic activities and association with p27Kip1: In agreement with the results of westernblot analysis, cyclin-D1 and -D2 associated kinases were activated soon after serum addition in a G1 phase-limited manner (Figure 14A). Since immunoprecipitation showed that p27Kip1 association with cyclin-D1 and

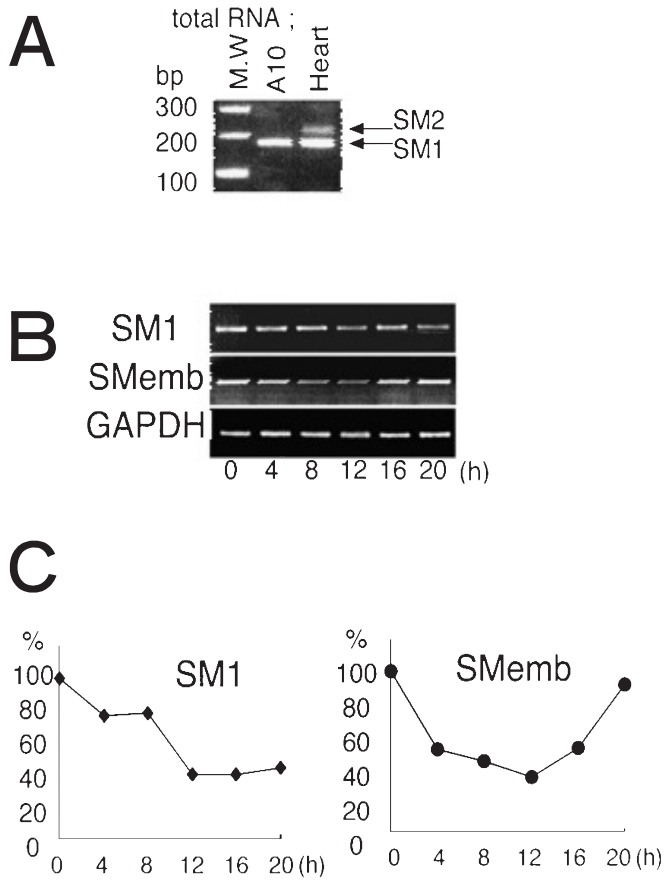

Figure 11 Alterations of SM-MHC, Non Muscle MHC expressions by mitogenic stimulation
A, Total RNA from A10 cells or adult rat heart were reverse transcribed, subjected to PCR to quantify SM1 or SM2 mRNA. B, Total RNA were extracted at every 4 hour and quantitative RT-PCRs were performed to measure each mRNA of SM1/2, SMemb, and GAPDH. C, Fluorescence intensities were quantified and expressed as relative values to those of GAPDH.

cyclin-D2 was parallel to the protein level of cyclin-D1, -D2 (Figure 13A, Figure 14B), it was unlikely that p27Kip1 acted as an inhibitor for cyclin-D1, -D2 associated kinases. Cyclin-E associated kinase was faintly activated during G1 phase, but significant activation was detected at G1/S transitional phase and this elevated level was sustained (Figure 14A) and then abruptly declined after 24 hours (Data not shown). p27Kip1 maximally associated to cyclin-E at G0/G1 phase but gradually disappeared from cyclin-E/CDK2 complex at G1 phase and we could never detect cyclin-E bound p27Kip1 protein during S phase (Figure 14B). Taken together,

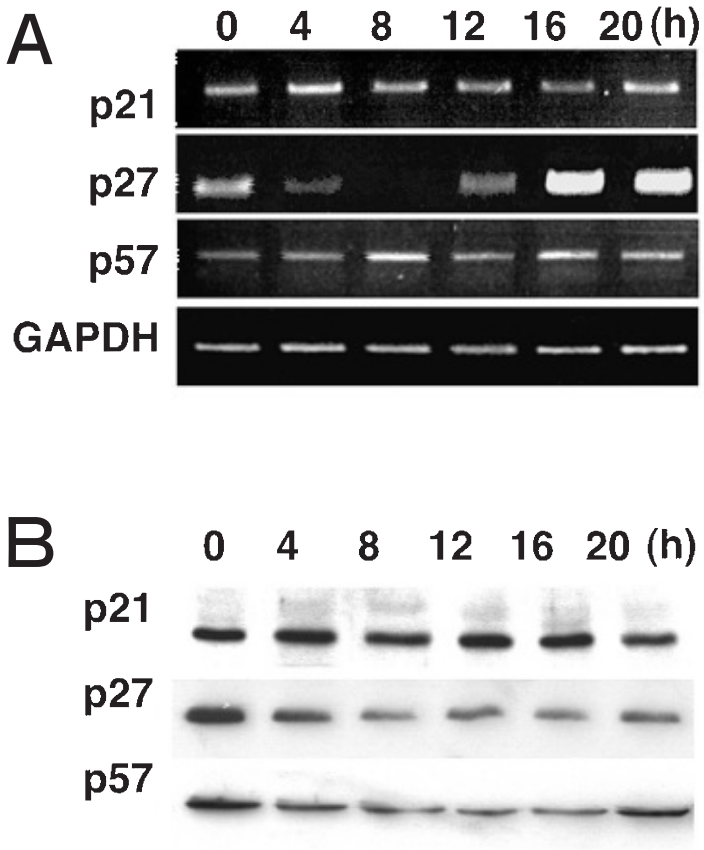

Figure 12 Alterations of protein and mRNA expression of p21Cip1 family after serum stimulation
A, RT-PCR was performed to quantify each CKI and GAPDH. B, Total cell lysates were harvested at every 4 hour, separated by SDS-PAGE (12% for p21 and p27, 10% for p57), blotted and incubated with polyclonal antibodies against p21, p27, and p57, respectively.

these results indicated that cyclin-E associated kinases was activated by the initial decline of p27Kip1 and sequential increase of both regulatory and catalytic units; cyclin-E and CDK2. The binding of p27Kip1 to cyclin-D may not be inhibitory in the course of immature VSMCs proliferation.

Rb family protein expression: As already reported, Rb family proteins are phosphorylated by cyclin/CDK complexes and hyperphosphorylated Rb proteins show the slower mobility shifts than non- and hypo- phosphorylated types on SDS-PAGE. Because there was no difference in Rb family expression and their phosphorylation with or without forcible expression of Ad-LacZ (data not shown), we show only the results of westernblot analysis of Ad-LacZ transfected A10 cells (Figure 15, left column). The phosphorylation of Rb itself was not so significant and remained unchanged. Rb protein expression was constant even after S phase entry. On the

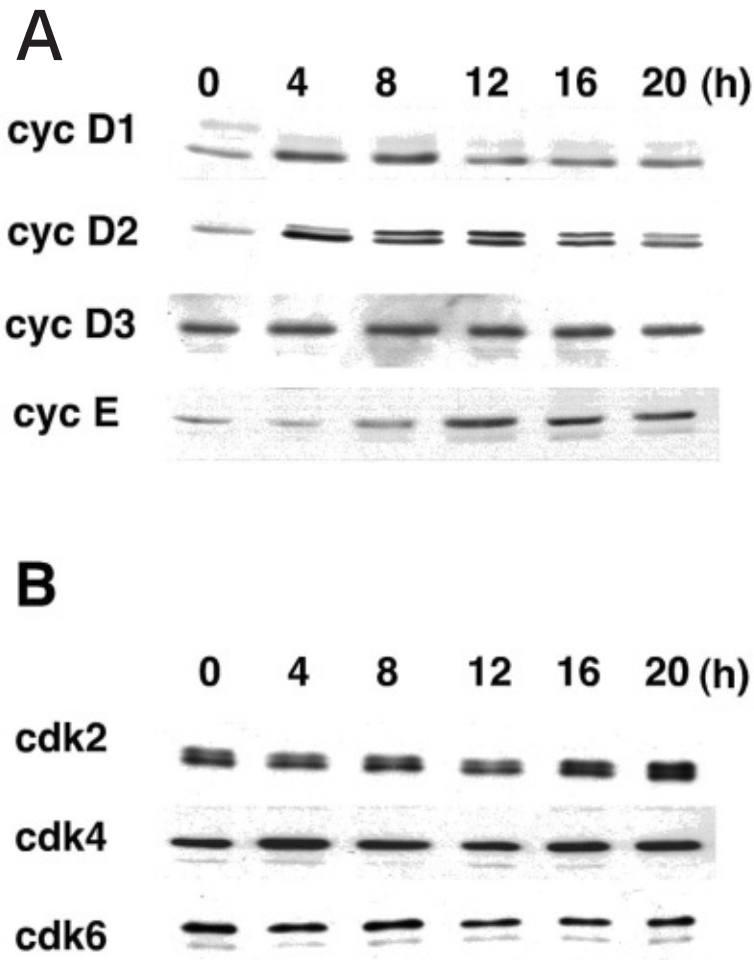

Figure 13 Alterations of G1 cyclin and CDK protein expressions after serum stimulation
G0 arrested A10 cells were stimulated with growth medium, harvested at every 4 hour, and total cell lysates were separated by SDS-PAGE. Blotted membranes were analyzed with specific antibodies against cyclin-D1, cyclin-D2, cyclin-D3, cyclin-E (A), and CDK2, CDK4, CDK6 (B).

other hand, both p107 and p130 demonstrated mobility shift toward the hyperphosphorylated forms at G1 phase. After S phase entry, p107 was highly phosphorylated and p130 abruptly degraded (Figure 15, left column).

p57 overexpression cancels the cyclin-D/CDK4 activation and Rb phosphorylation: It is well known that another family of CDK inhibitor, INK, exclusively binds to CDK4/6 preventing its association with cyclin-D and thereby inactivates CDK4/6. But in normal uninjured arteries, INK family proteins are barely detected[52), 70)] Although p15 and p16 are newly synthesized with the mitogenic stimulation in

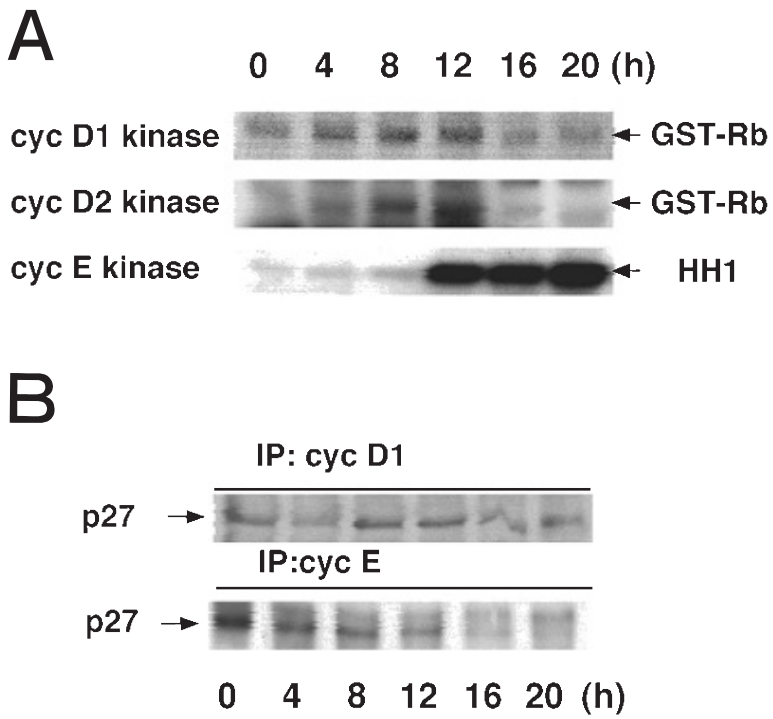

Figure 14 G1 cyclin/CDK complexes activation and their binding to p27Kip1 and p57Kip2
A, Total cell lysates were immunoprecipitated with anti-cyclin-D1, -D2, or cyclin-E antibodies, then kinase reactions were carried out using GST-Rb (for cyclin-D1, D2) or Histone H1 (for cyclin-E) as substrates. Labeled products were resolved on 10% SDS-PAGE and subjected to autoradiography. B, Immunoprecipitates with anti-cyclin-D1 or cyclin-E were resolved on SDS-PAGE, blotted and analyzed with anti-p27 polyclonal antibody.

primary cultured VSMCs, their expression level don't diminish throughout cell cycle progression[52), 70)] Thus, with regard to the activation of cyclin-D/CDK4 enzymes in immature SMC proliferation, INK family does not seem to be involved, nor does the p27Kip1 bound to cyclin-D, as stated before. We hypothesized that one of the triggers of cyclin-D/CDK4 activation might be p57Kip2 downregulation, in addition to the transient accumulation of cyclin-D1, -D2. Overexpression of p57Kip2 inhibited phosphorylation of all Rb family members and the elevation of p107 protein (Figure 15 right column). Furthermore, p57Kip2 could bind to cyclin-D1 and to a lesser extent, cyclin-E (Figure 15B). At that time, cyclin A bound p57 was undetectable, probably because Ad-p57 transfected cells were unable to enter S phase and to induce cyclin A expression. Finally, transient transfection of p57Kip2 effectively cancelled the activation of both cyclin-D1/CDK4 and cyclin-E/CDK2 (Figure 16).

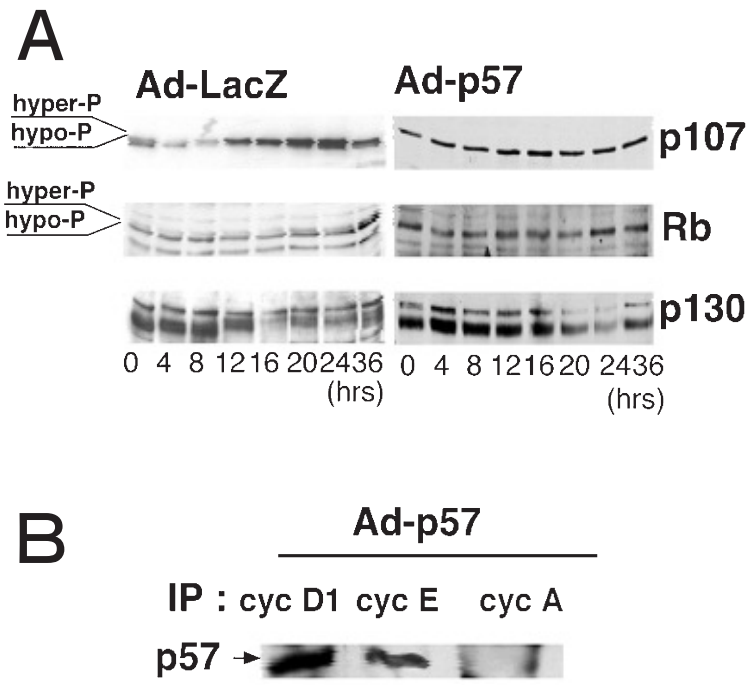

Figure 15 Overexpression of p57Kip2 suppressed the cyclin-D/CDK4 activation and Rb phosphorylation
A, After infection with Ad-LacZ or Ad-p57, cells were starved and stimulated with growth medium. Total cell lysates were separated by 6% SDS-PAGE, blotted with polyclonal anti-p107 and p130, or monoclonal anti-Rb antibody. B, Exponentially growing cells were infected with Ad-p57 for one hour and replaced with growth medium. After 48 hours incubation, immunoprecipitates with anti-cyclin-D1, cyclin-E or cyclin-A antibodies were resolved by SDS-PAGE, blotted with anti-p57 antibody.

Discussion

In several animal models, it has been shown that p27Kip1 is abundantly expressed in normal arteries, diminished soon after balloon injury, then upregulated as SMC begin to arrest[52] These findings suggest that p27Kip1 is likely to correlate inversely with SMC proliferation and to be one of the "threshold-establishing molecules". Indeed, forcible expression of p27Kip1 limited the neointimal formation after balloon denudation71 and p27Kip1 deficient mice exhibited increased body size with hypercellularity in multiple organs and enhanced cell proliferation in response to mitogenic stimulation[72] It has been known that p27Kip1 is a G1 specific CDK inhibitor and its overexpression causes G1 cell arrest. But, recent in vivo study suggested that p27Kip1 actively assemble cyclin-D and CDK4 in early G1 phase[73] Consistently, our findings also revealed that cyclin-D1 binding fraction of

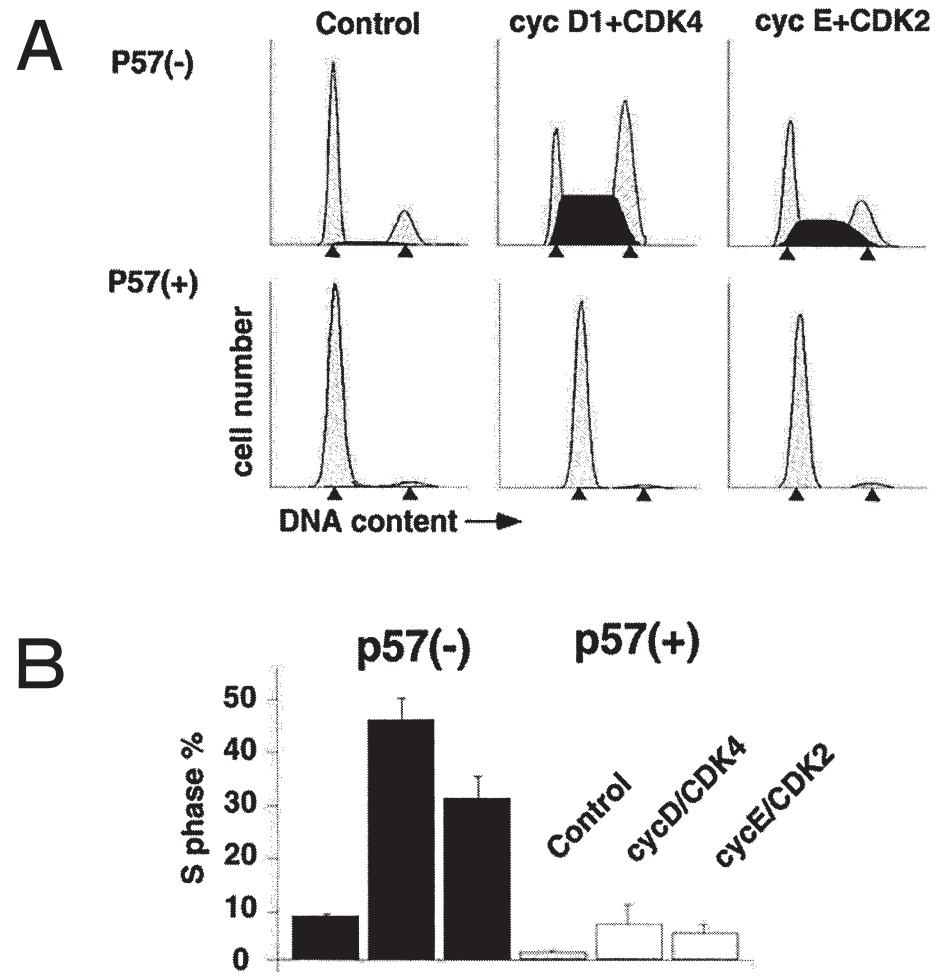

Figure 16 Effect of transiently expressed p57Kip2 on the cell cycle distribution of SMC

DNA histograms of CD20-positive cell populations in which relative DNA comtent is plotted against cell number. The cells were transfected with 2μg of pcDNA-CD20 in combination with 20μg of pcDNA vector (control), 10μg of pRCcyc D1 and 10μg of pcDNA-CDK4 (cyclin-D1/CDK4), 10μg of pRCcyc E and 10μg of pcDNA-CDK2 (cyclin-E/CDK2), 10μg of pcDNAp57 and 10μg of pcDNA (p57), 7μg of pRCcyc D1 and 7μg of pcDNA-CDK4 and 7μg of pcDNAp57 (cyclin-D1/CDK4/p57), 7μg of pRCcyc E and 7μg of pcDNA-CDK2 and 7μg of pcDNAp57 (cyclin-E/CDK2/p57). The cells were harvested 48 hours after the removal of DNA precipitates, stained for CD20 expression and DNA content, and analysed by flow cytometry.

p27Kip1 was accumulated rather than diminished at G1 phase, in contrast to its association with cyclin-E.

Quantitative RT-PCR indicated that p27Kip1 protein expression is regulated at transcriptional level. Recent report demonstrated that murine promoter region of

p27Kip1 contained potential binding sites for transcriptional factors including SP1, CRE, Myb, NFκB[74] In the process of immature SMC proliferation, these transcription factors might be involved in the regulation of p27Kip1 mRNA expression. Of course our findings do not deny the possibility of post-transcriptional regulation of p27Kip1 content, and a large body of studies are indicating the amount of p27Kip1 is also controlled by post-transcriptional pathway such as ubiquitination[75], and by binding E1A oncoprotein[76].

A10 cells constitutively expressed p21 even at G0/G1 arrested phase and the levels of p21Cip1 mRNA and protein were not reduced throughout our observation. But previous work has demonstrated that p21Cip1 is minimally expressed in normal arteries by westernblot or immunostaining[52), 53)], and unlike p27Kip1, p21Cip1 is upregulated when SMC cease to proliferate. Therefore, p21Cip1 acts as an "inducible growth inhibitor" against cell division in the later phase of arterial healing. So far, we can't find plausible explanation for the discrepancy between our observation and the previous reports. Considering A10 cells kept immature phenotype and did not differentiate under the pressure of serum deprivation, constant expression of p21Cip1 might suggest that A10 are already free from the growth inhibitory effect of p21Cip1, and able to maintain such dedefferentiated phenotype. Indeed, westernblot analysis revealed that primary cultured rat SMC upregulated the amount of p21Cip1 after mitogenic stimulation[77].

It is worth to mention that, from knockout mice studies of all p21 family members, only p57Kip2 gene elimination resulted in embryonic lethality and developmental abnormalities[78), 79)] The phenotypes of p57-null cell were inability to exit from cell cycle and inappropriate apoptosis during differentiation process. Similar characteristics were revealed in Rb targeted mice[80] Thus, in certain cell lineages, functional link is suggested between p57Kip2 and Rb in the cell differentiation. Surprisingly, by serum stimulation, differentiated skeletal muscle cells derived from Rb deficient mice can re-enter cell cycle and progress into S phase through hyperphosphorylation and rapid degradation of Rb-related protein, p107[81] This study may demonstrate that p107 could substitute Rb only for the induction of proliferation and differentiation in Rb lacking status, but not for the ability to maintain the terminal differentiation. This might be the case with our findings as shown in Figure 15A (left column). A10 doesn't differentiate after mitogenic stimulation and Rb hyperphosphorylation is not detected meanwhile. But, it does replicates and p107 is hyperphosphorylated. Although these are interesting consistency, it has not been elucidated how p107 and/or Rb are distinctively utilized in cell-cycle machinery.

In adult, p57Kip2 is highly expressed only in post-mitotic cells (brain, heart, skeletal muscle, lung and eye)[55] Furthermore, as presented in this study, p57Kip2 prevents G1 specific cyclin/CDK complexes from phosphorylating Rb proteins in immature SMC. Taken together, p57Kip2 seems to play two distinct roles depending on each developmental stage. At embryo, p57Kip2 controls the cell cycle

progression and withdrawal from that. But, in post-mitotic cells, p57Kip2 appears not to regulate cell proliferation, instead, it would commit the immature cells to a certain cell lineage, promote and maintain them into terminal differentiation.

While preparing this manuscript, a striking finding was reported by Dyer et al[82] They proposed two distinct roles of p57Kip2 in the development of mouce retina, as a CDK inhibitor in mitotic progenitor cells, and as a regulatory molecule of neuronal cell differentiation. Molecular markers of differentiation are expressed depending on SMC maturity[65), 83)] So far, there are two categories of phenotypic molecular markers, those for contractile "adult" SMC; SMα-actin, SM22, calponin, and for synthetic "pup" SMC; osteopontin, SM22 BMP2A, fibronectin ED-A, TF, and Smemb[65), 83)] SM-MHC has been well characterized in various clinical settings[65), 66)] In differentiated SMC, SM1 level is relatively high and also SM2 is expressed. On the contrary, in immature SMC, SM1 level is declined and SM2 is no more detectable, in turn, SMemb newly emerges[68)] In our experiments, SM2 expression was not detectable throughout observation and SMemb was constitutively expressed. Therefore, A10 SMC are specified as not well-differentiated or immature cell type. It is reported that immature SMC do exist even in adult uninjured arteries, and normal arterial media is composed of a mixture of different phenotypic smooth muscle cells[65), 83)] Hence, neointimal formation might be an expansion of a preexisting SMC subpopulation specifically prepared for repairing arterial wound. Although it remains to be proven where these subpopulation of cells are originated from, immature smooth muscle cells like A10 would be an appropriate target to test the feasibilities of molecular intervantional approach to prevent SMC proliferation. We have already confirmed that overexpression of p57Kip2 promotes the inhibition of [^{3}H] -thymidine incorporation and cell cycle arrest at G1, and moreover, adenovirus-mdiated overexpression of p57Kip2 prevents the development of neointimal hyperplasia of rabbit carotid artery after balloon denudation (manuscripts are in preparation). Taken together, our results suggest that p57Kip2 downregulation is not a by-stander phenomenon but one of the critical events for the initiation of immature SMC proliferation.

In conclusions, we demonstrated that p57kip2 and p27kip1 are constitutively expressed in G0 arrested immature SMC, After mitogenic stimulation, they coordinately decreased abruptly in correlation with the upragulation of cyclin-D, cyclin-E and CDK2, resulting in activation of cyclin-D and cyclin-E associated CDKs. Overexpression of p57kip2 significantly inhibited hyper-phosphorylation of all Rb family members by binding to both cyclin-D and cyclin-E complexes. These results suggested that the decline of p57kip2 protein level could be an initial trigger for G1-S progression in immature SMC. Futher investigation of p57kip2 function would provide useful information to control the cell cycle of SMC, and ultimately to prevent various vascular proliferative diseases including coronary restenosis after PCI.

5. Future prospect

Through these research, it has been cleared that cyclin-dependent kinase inhibitor, especially p27Kip1 and p57Kip2, are playing a pivotal role in the cell cycle control of vascular smooth muscle. Recently, rapamycin has been identified as one of the most promising agent for the prevention of coronary restenosis after percutaneous coronary intervention. Accumulating evidences suggest that the antiproliferative effect of rapamycin depends on its ability to regulate the stability of a cyclin-dependent kinase inhibitor (CKI), p27Kip1. Recently, we found that rapamycin completely inhibited the serum-induced down-regulation of both p57Kip2 and p27Kip1. Fluorescence microscopic observation showed that rapamycin significantly suppressed the serum-induced extra-nuclear translocation of EGFP-tagged p27Kip1. This finding suggested that rapamycin treatment disturbed the phosphorylation of nuclear p27Kip1, which is known as a critical step for the extra-nuclear translocation and degradation of this molecule. Sustained nuclear expression of p27Kip1 and cell-cycle arrest was also mimicked by the adenovirus-mediated overexpression of p57Kip2 in VSMC. These results suggested that p57Kip2 might be the prime target molecule of rapamycin, and also the key element for cell cycle control of vascular smooth muscle cells.

Further investugation regarding CKI would provide us a better understanding of the regulatory mechanism of cell cycle progression in cardiovascular system, and could lead to a new pharmacological intervention to treat the coronary restenosis and atherosclerosis in the near future.

6. Acknowledgments

The author thanks Drs. Noritsugu Nakano, Yasushi Takagi, Satoshi Kaneta, Takahiko Saito, Naotsugu Oyama and Hidetsugu Sakai, who provided great help to obtain the data in this chapter.

References

1. Kuntz RE, Baim DS. Defining coronary restenosis. Newer clinical and angiographic paradigms. *Circulation*. 1993; 88: 1310–1323
2. Erbel R, Haude M, Hopp HW. Coronary-artery stenting compaired with balloon angioplasty for restenosis after initial balloon angioplasty. Restenosis Stent Study Group. *N Engl J Med*. 1998; 339: 1672–1678
3. Libby P, Schwartz D, Brogi E, et al. A cascade model for restenosis. A special case of atherosclerosis progression. *Circulation*. 1992; 86 (6 Suppl): III47–III52
4. Seger R, Krebs EG. The MAPK signaling cascade. *FASEB J*. 1995; 9: 726–735
5. Schwartz L, Bourassa MG, Lesperance J, *et al*. Aspirin and dipyridamole in the prevention of restenosis after percutaneous transluminal coronary angioplasty. *N Engl J Med*. 1988; 318: 1714–1719
6. Schwartz L, Lesperance J, Bourassa MG, et al. The role of antiplatelet agents in modifying

the extent of restenosis following percutaneous transluminal coronary angioplasty. *Am Heart J*. 1990; 119: 232–236
7. Hoberg E, Kubler W. Prevention of restenosis after PTCA: role of calcium antagonists. *J Cardiovasc Pharmacol*. 1991; 18 Suppl 6:S15–S19
8. Faxon DP. Effect of high dose angiotensin-converting enzyme inhibition on restenosis: final results of the MARCATOR Study, a multicenter, double-blind, placebo-controlled trial of cilazapril. The Multicenter American Research Trial With Cilazapril After Angioplasty to Prevent Transluminal Coronary Obstruction and Restenosis (MARCATOR) Study Group. *J Am Coll Cardiol*. 1995; 25: 362–369
9. Bertrand ME, McFadden EP, Fruchart JC, et al. Effect of pravastatin on angiographic restenosis after coronary balloon angioplasty. The PREDICT Trial Investigators. Prevention of Restenosis by Elisor after Transluminal Coronary Angioplasty. *J Am Coll Cardiol*. 1997; 30: 863–869
10. Pepine CJ, Hirshfeld JW, Macdonald RG, et al. A controlled trial of corticosteroids to prevent restenosis after coronary angioplasty. M-HEART Group. *Circulation*. 1990; 81: 1753–1761
11. Kosuga K, Tamai H, Ueda K, et al. Effectiveness of tranilast on restenosis after directional coronary atherectomy. *Am Heart J*. 1997; 134: 712–718
12. Maresta A, Balducelli M, Cantini L, et al. Trapidil (triazolopyrimidine), a platelet-derived growth factor antagonist, reduces restenosis after percutaneous transluminal coronary angioplasty. Results of the randomized, double-blind STARC study. Studio Trapidil versus Aspirin nella Restenosi Coronarica. *Circulation*. 1994; 90: 2710–2715
13. Tardif JC, Cote G, Lesperance J, et al. Probucol and multivitamins in the prevention of restenosis after coronary angioplasty. Multivitamins and Probucol Study Group. *N Engl J Med*. 1997; 337(6): 365–372
14. Ross R. The pathogenesis of atherosclerosis: a perspective for the 1990 s. *Nature*. 1993; 362: 801–809
15. Hawking F. Suramin: With special reference to onchocerciasis. *Adv Phramacol Chemother*. 1978; 15: 289–322
16. Hosang M. Suramin binds to platelet-derived growth factor and inhibits its biological activity. *J Cell Biochem*. 1985; 29: 265–273
17. Coffey RJ Jr, Leof EB, Shipley GD, et al. Suramin inhibition of growth factor receptor binding and mitogenicity in AKR-2 B cells. *J Cell Physiol*. 1987; 132: 143–148
18. Coughlin SR, Barr PJ, Cousens LS, et al. Acidic and basic fibroblast growth factors stimulate tyrosine kinase activity in vivo. *J Biol Chem*. 1988; 263: 988–993
19. Pollak M, Richard M. Suramin blockade of insulinlike growth factor I-stimulated proliferation of human osteosarcoma cells. *J Natl Cancer Inst*. 1990; 82: 1349–1352
20. Baumann H, Strassmann G. Suramin inhibits the stimulation of acute phase plasma protein genes by IL-6-type cytokines in rat hepatoma cells. *J Immunol*. 1993; 151: 1456–1462
21. Hensey CE, Boscoboinik D, Azzi A. Suramin, an anti-cancer drug, inhibits protein kinase C and induces differentiation in neuroblastoma cell clone NB2A. *FEBS Lett*. 1989; 258: 156–158
22. Kopp R, Pfeiffer A. Suramin alters phosphoinositide synthesis and inhibits growth factor receptor binding in HT-29 cells. *Cancer Res*. 1990; 50: 6490–6496
23. Tsiquaye K, Zuckerman A. Suramin inhibits duck hepatitis B virus DNA polymerase activity. *J Hepatol*. 1985; 1: 663–669

24. Bojanowski K, Lelievre S, Markovits J, et al. Suramin is an inhibitor of DNA topoisomerase II in vitro and in Chinese hamster fibrosarcoma cells. *Proc Natl Acad Sci USA*. 1992; 89: 3025-3029
25. De Clercq E. Suramin: a potent inhibitor of the reverse transcriptase of RNA tumor viruses. *Cancer Lett*. 1979; 8: 9-22
26. Minniti CP, Maggi M, Helman LJ. Suramin inhibits the growth of human rhabdomyosarcoma by interrupting the insulin-like growth factor II autocrine growth loop. *Cancer Res*. 1992; 52: 1830-1835
27. Shiao RT, Miglietta L, Khera SY, et al. Dexamethasone and suramin inhibit cell proliferation and interleukin-6-mediated immunoglobulin secretion in human lymphoid and multiple myeloma cell lines. *Leuk Lymphoma*. 1995; 17: 485-494
28. Berns EM, Schuurmans AL, Bolt J, et al. Antiproliferative effects of suramin on androgen responsive tumor cells. *Eur J Cancer*. 1990; 26: 470-474
29. Vignon F, Prebois C, Rochefort H. Inhibition of breast cancer growth by suramin. *J Natl Cancer Inst*. 1992; 84: 38-42
30. Hosang M. Suramin binds to platelet-derived growth factor and inhibits its biological activity. *J Cell Biochem*. 1985; 29: 265-273
31. Foekens JA, Sieuwerts AM, Stuurman-Smeets EM, et al. Pleiotropic actions of suramin on the proliferation of human breast-cancer cells in vitro. *Int J Cancer*. 1992; 51: 439-444
32. Cardinali M, Sartor O, Robbins KC. Suramin, an experimental chemotherapeutic drug, activates the receptor for epidermal growth factor and promote growth of certain malignant cells. *J Clin Invest*. 1992; 89: 1242-1247
33. Asada Y, Tsuneyoshi A, Marutsuka K, et al. Suramin inhibits intimal thickening following intimal injury in the rabbit aorta in vivo. *Cardiovasc Res*. 1994; 28: 1166-1169
34. Gray TJ, Strauss BH, Hinek A. Inhibitory mechanisms by which suramin may attenuate neointimal formation after balloon injury. *J Cardiovasc Pharmacol*. 1999; 33: 960-971
35. Edwards G, Breckenridge AM. Clinical pharmacokinetics of anthelmintic drugs. *Clin Pharmacokinet*. 1988; 15: 67-93
36. Gagliardi AR, Taylor MF, Collins DC. Uptake of suramin by human microvascular endothelial cells. *Cancer Lett*. 1998; 125: 97-102
37. Lincoff AM, Topol EJ, Ellis SG. Local Drug Delivery for the Prevention of Restenosis. *Circulation*. 1994; 90: 2070-2084
38. Wei GL, Krasinski K, Kearney M, et al. Temporally and Spatially Coordinated Expression of Cell Cycle Regulatory Factor After Angioplasty. *Circ Res*. 1997; 80: 418-426
39. Tanner FC, Yang Z, Duckers E, et al. Expression of Cyclin-Dependent Kinase Inhibitors in Vascular Disease. *Circ Res*. 1997; 82: 396-406
40. Yang Z, Simari RD, Perkins ND, et al. Role of the p21 cyclin-dependent kinase inhibitor in limiting intimal cell proliferation in response to arterial injury. *Proc Nattl Acad Sci*. 1996; 93: 7905-7910
41. Lee MH, Reynisdottir I, Massague J. Cloning of p57Kip2, a cyclin-dependent kinase inhibitor with unque domain structure and tissue distribution. *Genes & Dev*. 1995; 9: 639-649
42. Yan Y, Frisen J, Lee M, et al. Ablation of the CDK inhibitor p57kip2 resulta in increased apoputosis and delayed differentiation during mouse developement. *Genes & Development*. 1997; 11: 973-983
43. Deng C, Zhang P, Harper JW, et al. Mice Lacking p21cip1/waf1 Undergo Nomal Development, but Are Defective in G1 checkpoint Control. *Cell*. 1995; 82: 675-684

44. Nakayama K, Ishida N, Shirane M, et al. Mice Lacking p27kip1 Display Increased Body Size, Multiple Organ Hyperplasia, Retinal Dysplasia, and Pituitary Tumors. *Cell*. 1996; 85: 707-720
45. Sherr CJ. G1 phase progression: cycling on cue. *Cell*. 1994; 79: 551-555
46. Sherr CJ. Cancer cell cycles. *Science*. 1996; 274: 1672-1677
47. Morgan DO. Principles of CDK regulation. *Nature*. 1995; 374: 131-134
48. Sherr CJ, Roberts JM. Inhibitors of mammalian G1 cyclin-Dependent kinases. *Genes Dev*. 1995; 9: 1149-1163
49. Serrano M, Hannon GJ, Beach D. A new regulatory motif in cell-cycle control causing specific inhibition of cyclin-D/CDK4. *Nature*. 1993; 366: 704-707
50. Chellappan SP, Giordano A, Fisher PB. Role of cyclin-Dependent kinases and their inhibitors in cellular differentiation and development. *Curr Top Microbiol Immunol*. 1998; 227: 57-103
51. Harper JW, Elledge SJ, Keyomarsi K, et al. Inhibition of cyclin-Dependent kinases by p21. *Mol Biol Cell*. 1995; 6: 387-400
52. Tanner FC, Yang Z-Y, Duckers E, et al. Expression of cyclin-Dependent kinase inhibitors in vascular disease. *Circ Res*. 1999; 82: 396-403
53. Yang Z-Y, Shimari RD, Perkins ND, et al. Role of p21 cyclin-Dependent kinase inhibitor in limiting intimal cell proliferation in response to arterial injury. *Proc Natl Acad Sci*. 1996; 93: 7905-7910
54. Polyak K, Lee MH, Erdjument-Bromage H, et al. Cloning of p27kip1, a cyclin-Dependent kinase inhibitor and potential mediator of extracellular antimitogenic signals. *Cell*. 1994; 78: 59-66
55. Lee MH, Reynisdottir I, Massague J. Cloning of p57kip2, a cyclin-Dependent kinase inhibitor with unique domain structure and tissue distribution. *Genes Dev*. 1995; 9: 639-649
56. Matsuoka S. Edwards M, Bai C, et al. P57kip2, a structually distinct member of the p21cip1 CDK inhibitor family, is a candidate tumor supressor gene. *Genes Dev*. 1995; 9: 650-662
57. Reynaud EG, Pelpel K, Guillier M, et al. P57kip2 stabilizes the MyoD protein by inhibiting cyclin-E/CDK2 kinase activity in growing myoblasts. *Mol Cell Biol*. 1999; 19: 7621-7629
58. Reynaud EG, Leibovitch MP, Tintignac LA, et al. Stabilization of MyoD by direct binding to p57kip2. *J Biol Chem*. 2000; 275: 18767-18776
59. Harlow E, Lane D. Antibodies: a laboratory manual. 1988 cold spring harbor laboratory press.
60. Kimes BW, Brandt BL. Characterization of two putative smooth muscle cell lines from rat thoracic aorta. *Exp Cell Res*. 1976; 98: 349-366
61. Husain M, Bein K, Jiang L, et al. c-Myb dependent cell cycle progression and Ca2+storage in cultured vascular smooth muscle cells. *Circ Res*. 1997; 80: 617-626
62. Yu SM, Cheng ZJ, Guh JH, et al. Mechanism of anti-proliferation caused by YC-1, an indazole derivative, in cultured rat A10 vascular smooth-muscle cells. *Biochem J*. 1995; 306: 787-792
63. Rio MD, Sunkel C, Larcher F, et al. Antiproliferative effects of PCA-4230, a new antithrombotic drug, in vascular smooth muscle cells. *British J Pharma*. 1997; 120: 1360-1366
64. Rao RS, Miano JM, Olson E, et al. The A10 cell line: a model for neonatal, neointimal, or differentiated vascular smooth muscle cells? *Cardiovasc Res*. 1997; 36: 118-126
65. Schwartz SM, deBlois D, O'brien ERM. The intima: Soil for atherosclerosis and restenosis. *Circ Res*. 1995; 77: 445-465
66. Aikawa M, Sivam PN, Kuro-o M, et al. Human smooth muscle myosin heavy chain isofor-

ms as molecular markers for vascular develoment and atherosclerosis. *Circ Res*. 1993; 73: 1000-1012
67. Babij P, Periasamy M. Myosin heavy chain isoform diversity in smooth muscle is produced by differential RNA processing. *J Mol Biol*. 1989; 210: 673-679
68. Rovner AS, Murphy RA, Owens GK. Expression of smooth muscle myosin heavy chains in cultured vascular smooth muscle cells. *J Biol Chem*. 1986; 261: 14740-14745
69. Kuro-o M, Nagai R, Nakahara K, et al. cDNA cloning of a myosin heavy chain isoform in embryonic smooth muscle and its expression during vascular development and in artheriosclerosis. *J Biol Chem*. 1991; 266: 3768-3773
70. Olson NE, Kozlowski J, Reidy MA. Proliferation of intimal smooth muscle cells. *J Biol Chem*. 2000; 275: 11270-11277
71. Chen DC, Krasinski K, Chen D, et al. Downregulation of cyclin-Dependent kinase 2 activity and cyclin A promoter activity in vascular smooth muscle cells by p27kip1, and inhibitor of neointima formation in the rat carotid artery. *J Clin Invest*. 1997; 99: 2334-2341
72. Fero ML, Rivkin M, Tasch M. A syndrome of multiorgan hyperplasia with features of gigantism, tumorgenesis, and female sterility in p27kip1-deficient mice. *Cell*. 1996; 85: 733-744
73. Cheng M, Olivier P, Diehl JA, et al. The p21cip1 and p27kip1 CDK "inhibitors" are essential activators of cyclin-D-dependent kinases in murine fibroblasts. *EMBO J*. 1999; 18: 1571-1583
74. Kwon TK, Nagel JE, Buchholz MA, et al. Characterization of the murine cyclin-Dependent kinase inhibitor gene p27kip1. *Gene*. 1996; 180: 113-120
75. Pagano M, Tam SW, Theodoras AM, et al. Role of ubiquitin-proteasome pathway in regulating abundance of cyclin-Dependent kinase inhibitor p27. *Science*. 1995; 269: 682-685
76. Liu M, Lee M-H, Cohen M, et al. Transcriptional activation of the CDK inhibitor p21 by vitamin D3 leads to the induced differentiation of the myelomonocytic cell line U937. *Genes Dev*. 1996; 10: 142-153
77. Takahashi A, Taniguchi T, Ishikawa Y, et al. Trasilast inhibits vascular smooth muscle cell growth and intimal hyperplasia by induction of p21 and p53. *Circ Res*. 1999; 84: 543-550
78. Yan Y, Frisen J, Lee M-H, et al. Ablation of the CDK inhibitor p57kip2 results in increased apoptosis and delayed differentiation during mouce development. *Genes Dev*. 1997; 11: 973-983
79. Zhang P, Wong C, DePinho R, et al. Cooperation between the CDK inhibitors p27kip1 and p57kip2 in the control of tissue growth and devlopment. *Genes Dev*. 1998; 12: 3162-3167
80. Morgenbesser SD, Williams BO, Jacks T, et al. P53-dependent apoptosis produced by Rb-deficiency in the developing mouce lens. *Nature*. 1994; 371: 72-74
81. Schneider JW, Wei G, Liang Z, et al. Reversal terminal differentiation mediated by p107 in Rb-/- muscle cells. *Science*. 1994; 264: 1467-1471
82. Dyer MA, Cepko CL. P57kip2 regulates progenitor cell proliferation and amacrine interneuron development in the mouce retina. *Development*. 2000; 127: 3593-3605
83. Gittenberger-de Groot A, Deruiter MC, Bergwerff M, et al. Smooth muscle cell origin and its relation to heterogeneity in development and disease. *Arterioscler Thromb Vasc Biol*. 1999; 19: 1589-1594
84. Urasawa K, Kaneta S, Nakano N, et al. Vascular smooth muscle cell proliferation is effectively suppressed by the non-specific growth factor inhibitor suramin. Jpn Heart J. 2001; 42: 221-233